Computational Simulations of Electric Propulsion Aircraft: the X-57 Maxwell

Jared C. Duensing, Jeffrey A. Housman, Daniel Maldonado, James C. Jensen, Cetin C. Kiris

NASA Ames Research Center

Seung Y. Yoo

NASA Armstrong Flight Research Center

AMS Seminar Series, June 13th, 2019

NASA Ames Research Center, Moffett Field, California

Outline

- Introduction
  - X-57 CFD task overview
  - Motivation
- Part I: Computational simulations without propulsion
  - Establishing CFD Best Practices
    - Grid generation
    - Mesh refinement study
    - Numerical methods
    - Wind tunnel validation study
  - Power-Off Aerodynamic Database Results
- Part II: Computational simulations with propulsion
  - Cruise Power-On Database
  - High-Lift Power-On Database
- Summary

***Image source**: https://www.nasa.gov/press-release/nasa-electric-research-plane-gets-x-number-new-name*

Evolution of the X-57

NASA aims to achieve a 5X reduction in energy consumption for a private plane cruising at 150 knots through the latest X-57 design.

LeapTech Experiment

Demonstrated that distributed propulsion could provide nearly a 2X increase in lift relative to a traditional wing and propulsion system.

Mod-II

Proved the feasibility of two electrically driven propellers in place of traditional combustion engines.

Mod-III/Mod-IV

Combines distributed propulsion technology with electrically powered propellers. Mod-III studies the cruise propellers only, Mod-IV studies the high-lift propellers only.

X-57 Design Overview

Image source:
https://ntrs.nasa.gov/archive/nasa/casi.ntrs.nasa.gov/20170001218.pdf

Video source: *https://www.youtube.com/watch?v=4X1FxZgfFbc*

Objectives

- Establish best-practices to generate an aerodynamic database using the LAVA (Launch Ascent and Vehicle Aerodynamics) and Star-CCM+ flow solvers
- These best-practices are being applied to CFD databases which cover a variety of flight conditions
  - Database 1 (188 simulations): Power-off
    Database 2 (233 simulations): Cruise power-on
  - Database 3 (1000+ simulations): high-lift power-on
- The database results will be used to design the flight simulator and control systems for the aircraft

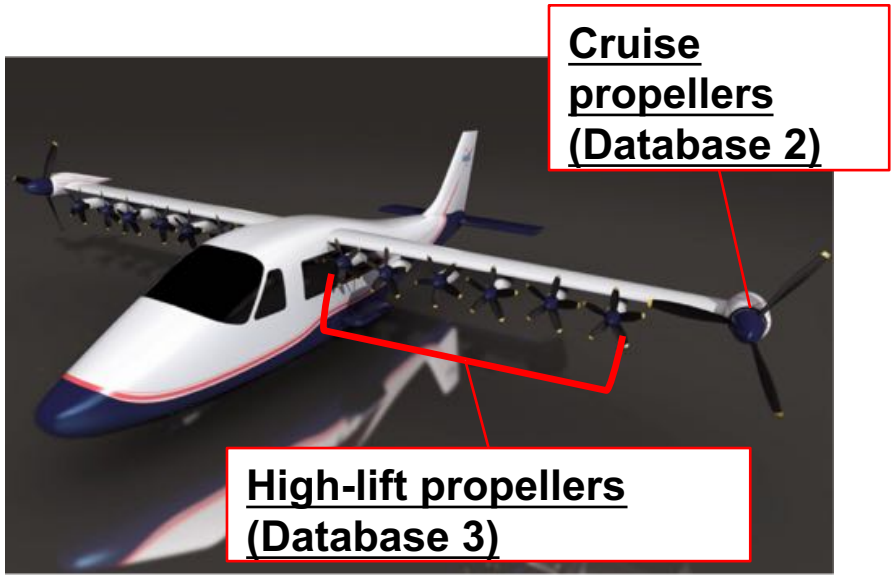

Steps to Establish Best-Practices Towards X-57 Database

1. Initial grid generation (structured curvilinear and unstructured polyhedral)
2. Free-air mesh refinement study
3. Study effects of:
   a. Low Mach Number Preconditioning
   b. Turbulence Model
   c. Numerical dissipation has been studied
4. Wind tunnel validation studies

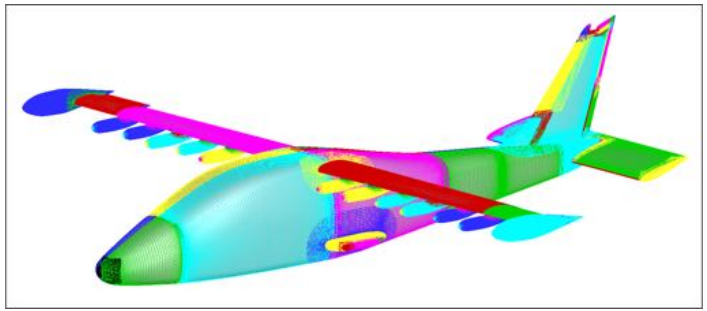

Sample X-57 structured overset grid

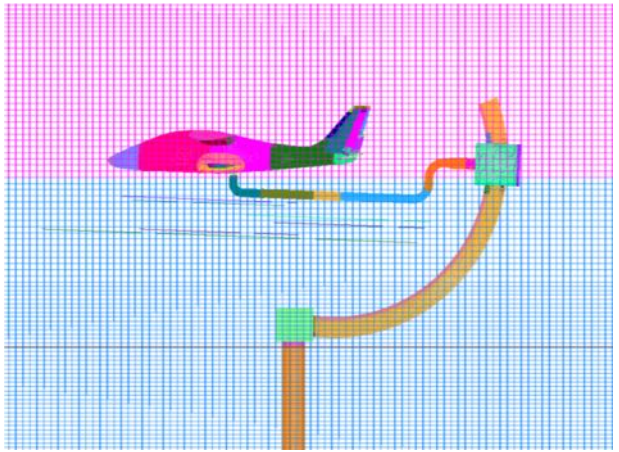

Sample X-57 structured overset grid in wind tunnel

Outline

- Introduction
  - X-57 CFD task overview
  - Motivation
- Part I: Computational simulations without propulsion
  - Establishing CFD Best Practices
    - Grid generation
    - Mesh refinement study
    - Numerical methods
    - Wind tunnel validation study
  - Power-Off Aerodynamic Database Results
- Part II: Computational simulations with propulsion
  - Cruise Power-On Database
  - High-Lift Power-On Database
- Summary

Structured Curvilinear Grid Generation (Ames LAVA Team)

- Mesh generation for this geometry occurs in three steps
  - CAD preparation and clean-up using ANSA (http://www.beta-cae.com/ansa.htm)
  - Structured patch construction in ANSA and Pointwise (http://www.pointwise.com/products/index.html)
  - Hyperbolic marching for more complex grids in Chimera Grid Tools (CGT)
  - Hyperbolic volume growth in CGT
  - Domain connectivity using combination of DCF module in OVERFLOW and LAVA modified implicit hole offset procedure

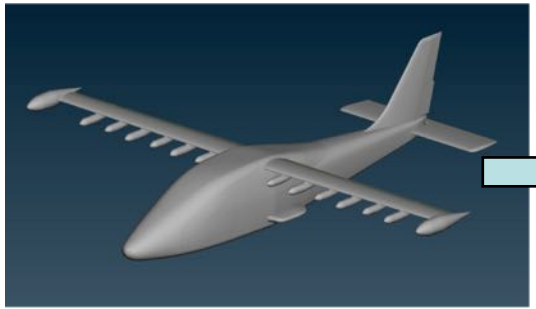

X-57 wind tunnel scale CAD model

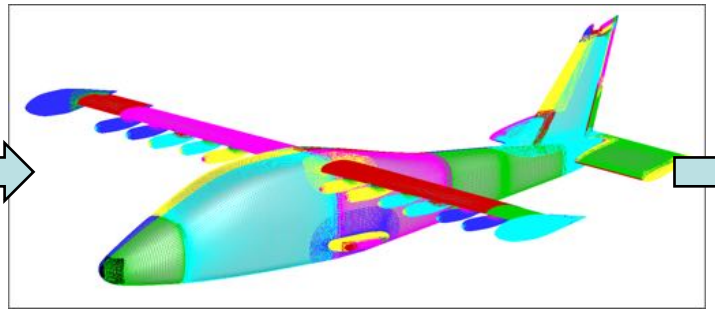

Surface geometry discretized into structured overset grids

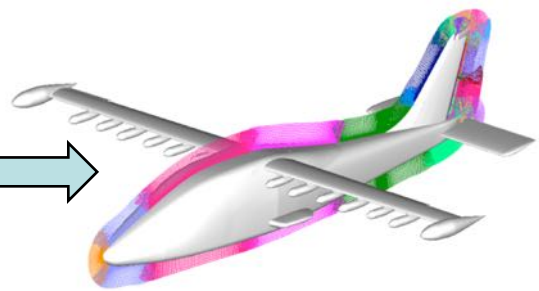

Surface geometry discretized into st overset grids

Grid Generation Guidelines

- Guidelines established by the High-Lift Prediction Workshop 3 (HLPW-3) were used to develop the initial grid system for the pre-database studies
  - Stretching ratio < 1.25
  - Leading edge spacing of 0.1% of the local chord
  - 5 points on all finite-thickness trailing edges
  - Double fringe minimum overlap
- ”Coarse” resolution targeted for initial grid for ease in consistent grid refinements
- Special procedure developed to generate grids over moving components

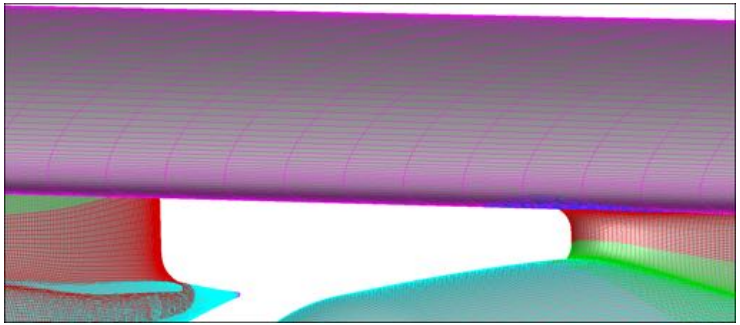

Wing leading edge (pink)

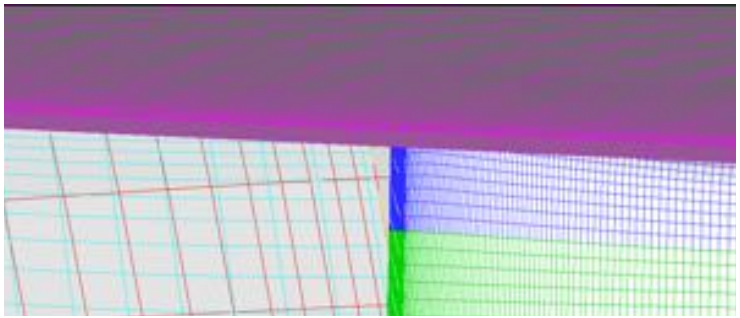

Wing trailing edge (pink)

Mesh Procedure for Moving Geometry

- Future database runs require the articulation of control surfaces to a specified angle
- A surface grid generation procedure was developed in which quadratic Bezier curves join open surfaces following a deflection

$$\vec{B}(t) = (1-t)^2\vec{P}_0 + 2(1-t)t\vec{P}_1 + t^2\vec{P}_2$$

δ_a= +10º

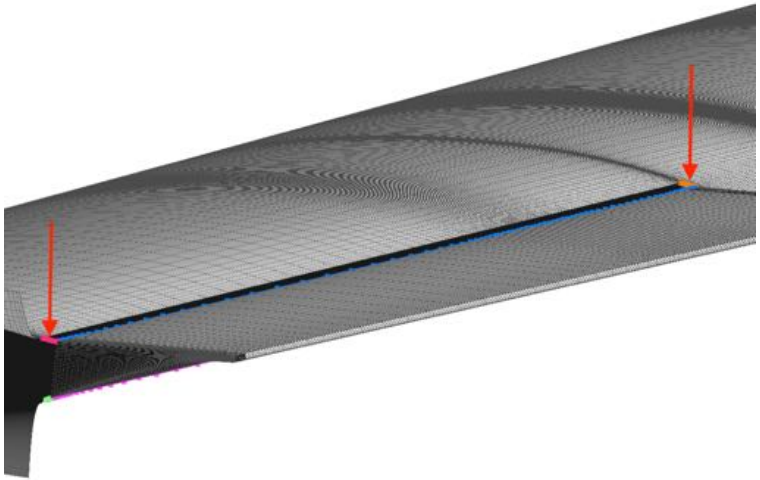

δ_a= -10º

Mesh Procedure for Moving Geometry

- Transfinite interpolation was then used to construct the control surface patch
- The resulting surface was then grown hyperbolically onto adjacent grids to create double fringe overlap

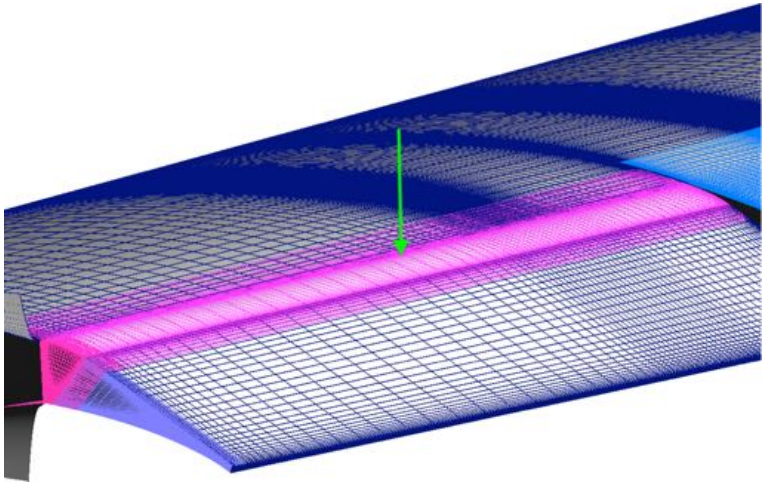

δ_a= +10º

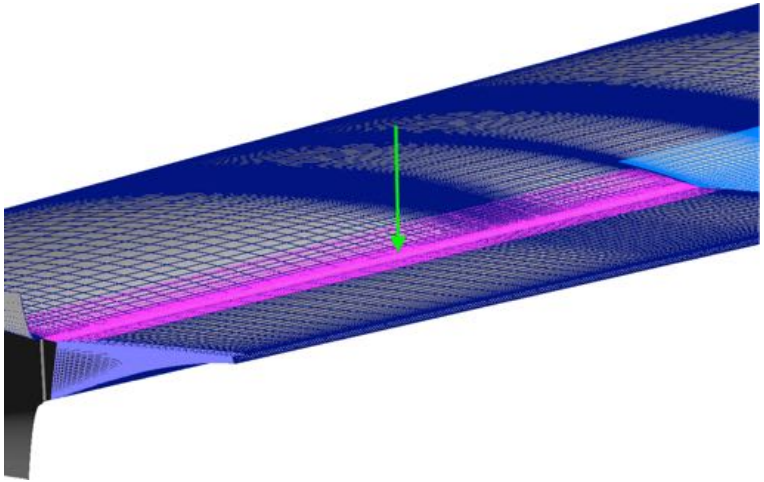

δ_a= -10º

Unstructured Grid Generation (AFRC CFD Team)

- Spacing and stretching guidelines for surface mesh generation similar to structured curvilinear grids
- Volume mesh grown using prismatic cells in the boundary layer and arbitrary polyhedral cells in the far-field

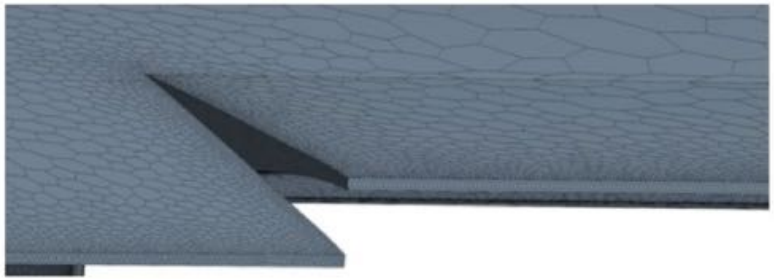

Aileron

Empennage

Outline

- Introduction
  - X-57 CFD task overview
  - Motivation
- Part I: Computational simulations without propulsion
  - Establishing CFD Best Practices
    - Grid generation
    - Mesh refinement study
    - Numerical methods
    - Wind tunnel validation study
  - Power-Off Aerodynamic Database Results
- Part II: Computational simulations with propulsion
  - Cruise Power-On Database
  - High-Lift Power-On Database
- Summary

Solver Details

- LAVA (Launch Ascent and Vehicle Aerodynamics) Curvilinear would be the primary flow solver used for this study with the commercial solver Star-CCM+ also used for comparison

Structured Curvilinear (LAVA)

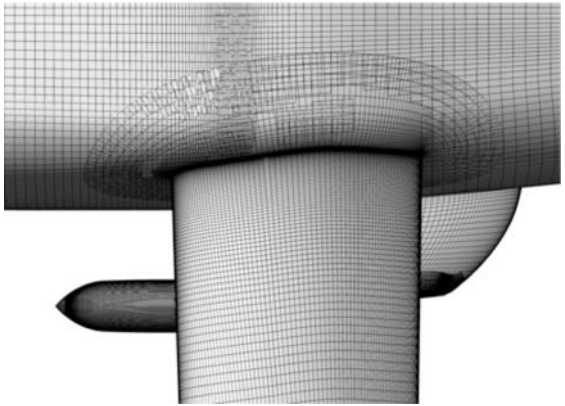

- Node-based steady-state RANS
- Second-order Roe convective flux discretization
- Van Albada flux limiter
- Spalart-Allmaras (SA) turbulence model with RC and QCR-2000

Unstructured Arbitrary Polyhedral (Star-CCM+)

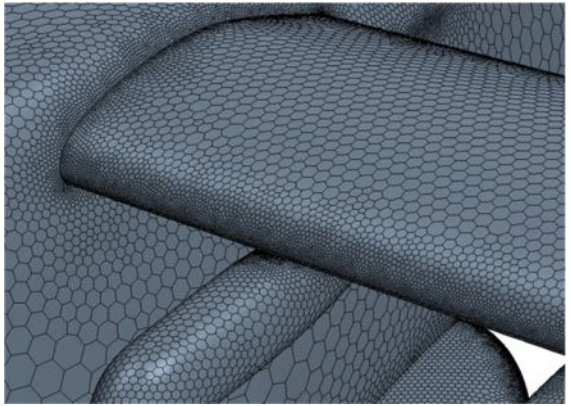

- Cell-centered steady-state RANS
- Second-order Roe convective flux discretization
- Venkatakrishnan flux limiter
- Spalart-Allmaras (SA) turbulence model with RC

Mesh Refinement Study Grid Statistics

Structured Curvilinear

Mesh	Grid Points	# of Zones
Coarse	80.0 M	315
Medium	159 M	315
Fine	322 M	315

Unstructured Arbitrary Polyhedral

Mesh	Grid Points
Coarse	17.2 M
Medium	49.7 M
Fine	120 M

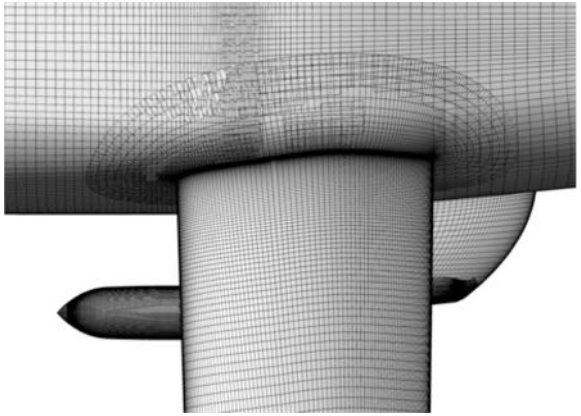

Structured Coarse

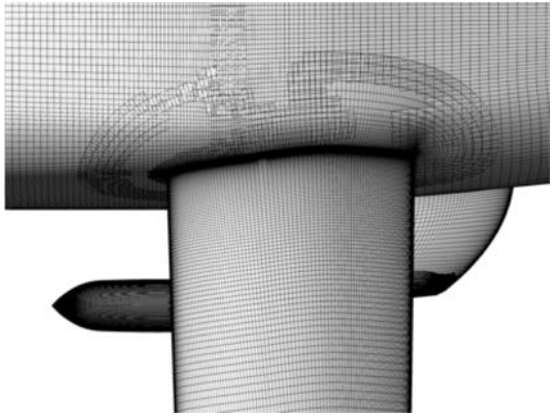

Structured Medium

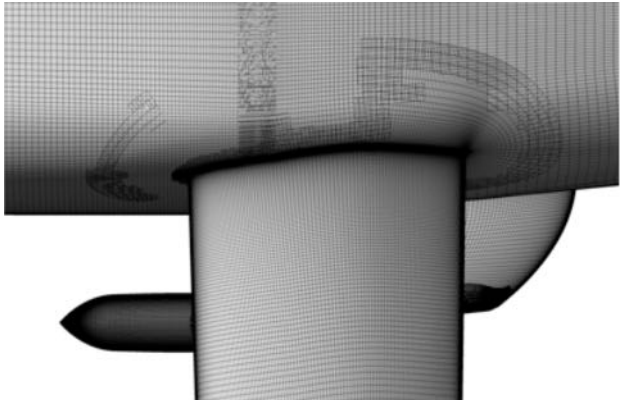

Structured Fine

Mesh Refinement Reference Conditions

- Case selected based on experimental data collected in the 12-foot low-speed wind tunnel at NASA Langley Research Center
- **Objective:** Use this condition and experimental data to determine appropriate solver settings and grid refinement level for future simulations

Quantity	Value
Mach Number	0.052
Reynolds Number (based on MAC)	121,600
Reference Static Temperature	288.1 K
Angle of Attack	6.0 º
Sideslip Angle	5.0 º
Aileron Deflection*	-10.0 º
Rudder Deflection*	-15.0 º
Stabilator Deflection*	-7.5 º

**Negative value corresponds to a trailing edge up (right for rudder) deflection*

Selecting Mesh Refinement Levels

- Second-order asymptotic convergence observed for drag, with the extrapolated drag for an "infinitely fine" grid within 1.1% error relative to other solver

	LAVA Curvilinear		Star-CCM+	
Grid	***CL***	***CD***	***CL***	***CD***
Coarse	1.0072	0.1138	1.0867	0.1274
Medium	1.0070	0.1121	1.0599	0.1198
Fine	1.0070	0.1115	1.0122	0.1152
Experiment	1.068	0.099	1.068	0.099

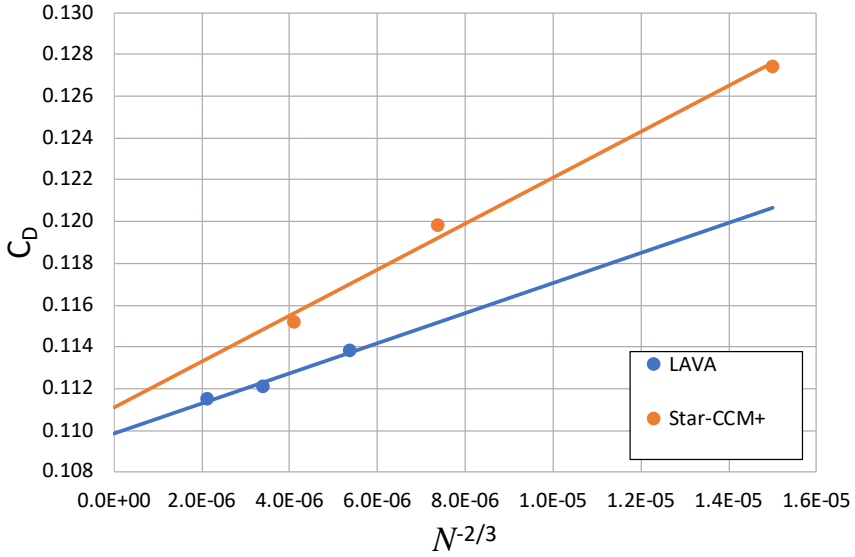

Pressure Distribution at Selected Wing Location

- Closer analysis of the pressure distribution at selected wing locations show strong agreement across all three refinement levels
- Virtually no change in pressure distribution between medium and fine levels

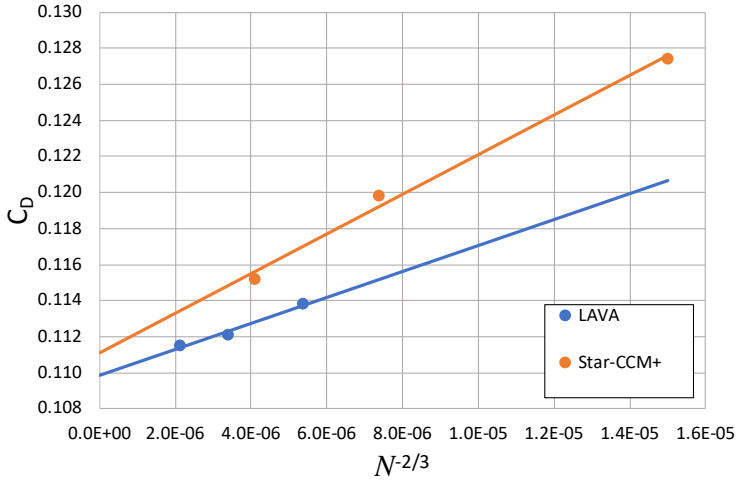

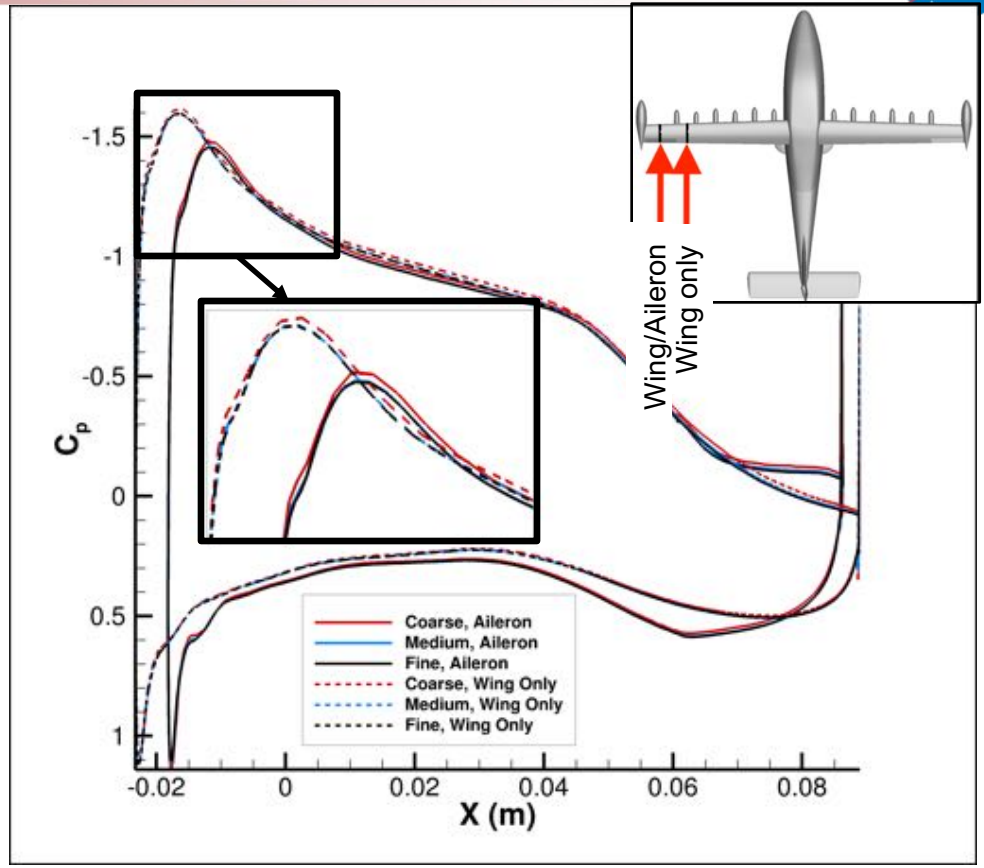

Outline

- Introduction
  - X-57 CFD task overview
  - Motivation
- Part I: Computational simulations without propulsion
  - Establishing CFD Best Practices
    - Grid generation
    - Mesh refinement study
    - Numerical methods
    - Wind tunnel validation study
  - Power-Off Aerodynamic Database Results
- Part II: Computational simulations with propulsion
  - Cruise Power-On Database
  - High-Lift Power-On Database
- Summary

Selecting Proper Solver Settings for LAVA

- Numerical discretization is a second-order convective flux scheme with van Albada slope limiter
- Coarse level grid was used to determine whether flow is best modeled fully turbulent or fully laminar (unless determined necessary, transitional flow would not be modeled)
- Effects of low-Mach preconditioning would be tested due to low speed flow
- Additional LAVA Unstructured simulations were also run to ensure consistency of solver settings within the LAVA framework

	LAVA Curvilinear		LAVA Unstructured	
Modeling Approach	***CL***	***CD***	***CL***	***CD***
Laminar without Preconditioning	0.579	0.151	1.016	0.171
Laminar with Preconditioning	0.585	0.146	0.664	0.160
SA Turbulence without Preconditioning	1.015	0.119	1.112	0.154
SA Turbulence with Preconditioning	1.007	0.114	1.066	0.125
Experiment	1.068	0.099	1.068	0.099

Outline

- Introduction
  - X-57 CFD task overview
  - Motivation
- Part I: Computational simulations without propulsion
  - Establishing CFD Best Practices
    - Grid generation
    - Mesh refinement study
    - Numerical methods
    - Wind tunnel validation study
  - Power-Off Aerodynamic Database Results
- Part II: Computational simulations with propulsion
  - Cruise Power-On Database
  - High-Lift Power-On Database
- Summary

Approaches to Minimize CFD Error

- Medium grid for both mesh paradigms was determined to be sufficiently fine based on lift and drag values relative to converged values
- Error relative to experiment appears to be reduced as much as possible due to modeling and mesh variations
- Other possible sources of error relative to experiment due to uncorrected experimental data provided
  - Wind tunnel wall interference
  - Buoyancy effects
  - Mounting fixture interaction
- A component build-up is desired to verify this theory and improve validation results

Image courtesy of Gerald Lee Pollard, NASA Langley Research Center

Wind Tunnel Validation Reference Conditions

- Case selected based on experimental data collected in the 12-foot low-speed wind tunnel at NASA Langley Research Center
- **Objective:** Perform CFD simulations of increasing fidelity to reduce error relative to experiment for validation cases

Quantity	Value
Mach Number	0.052
Reynolds Number (based on MAC)	121,600
Reference Static Temperature	288.1 K
Angle of Attack	2.0 º
Sideslip Angle	0.0 º
Aileron Deflection	0.0 º
Rudder Deflection	0.0 º
Stabilator Deflection	-15.0 º

Wind Tunnel Validation

- Component build-up incorporates wind tunnel hardware into the CFD simulation that could potentially influence aircraft loading

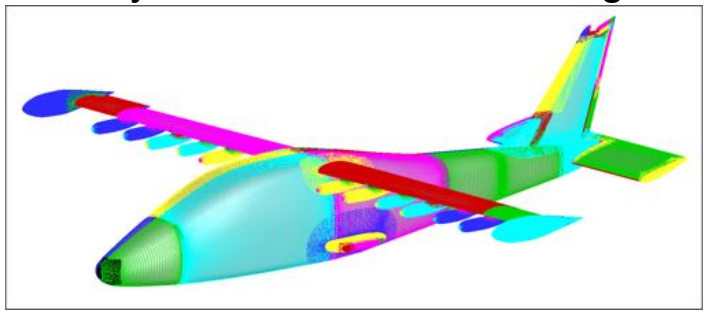

Free air: Baseline simulation approach used in refinement study.

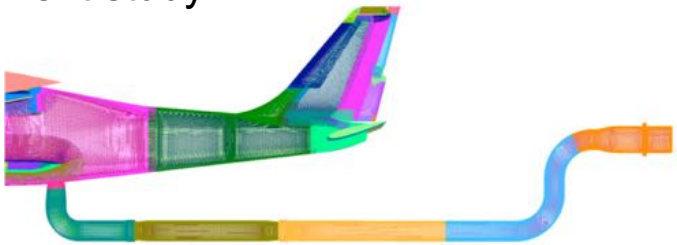

Free air + sting: Adds the sting mounting fixture to the free air simulation.

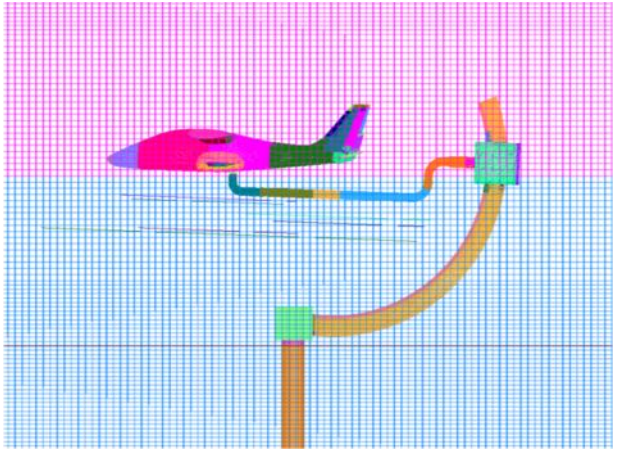

Free air + sting + wind tunnel: Adds the C-strut mount and encloses the aircraft in a 12 ft. x 12 ft. octagonal channel similar to the low-speed test section.

Wind Tunnel Validation

- Tunnel simulation designed to emulate blockage effects of wind tunnel hardware
- Test-section geometry extended 50 body lengths upstream and downstream (excludes inlet, diffuser, and surrounding recirculation chamber)

Image source:
https://researchdirectorate.larc.nasa.gov/12-foot-low-speed-tunnel-12-ft-lst/

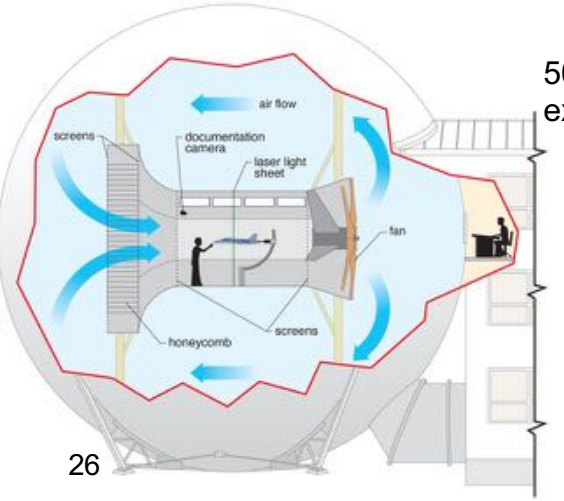

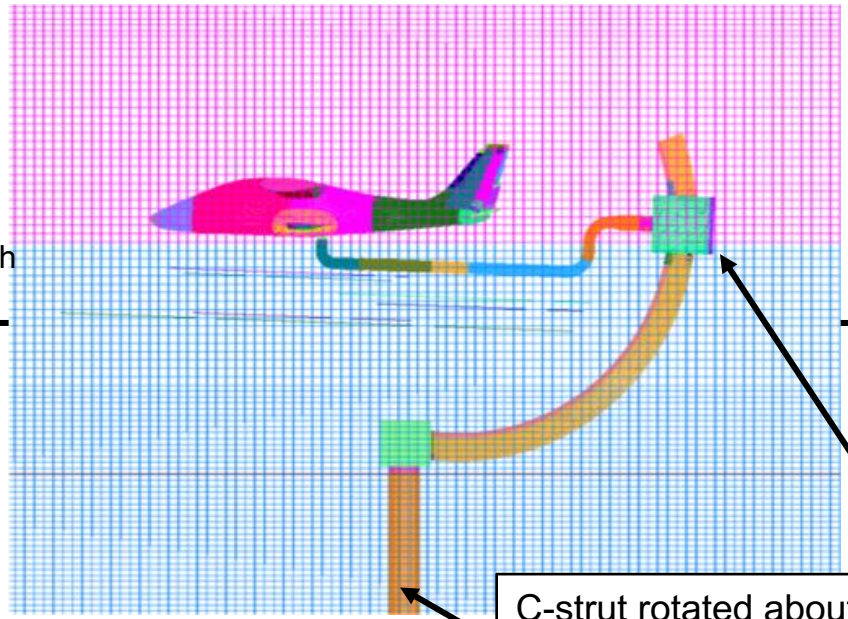

Validation Simulation Results (U-Velocity (m/s) on Symmetry Plane)

- Substantial qualitative differences in fluid dynamics resulting from sting, C-strut and wind tunnel walls
- Hardware locally impacts flow field while effects also propagate upstream to test article location

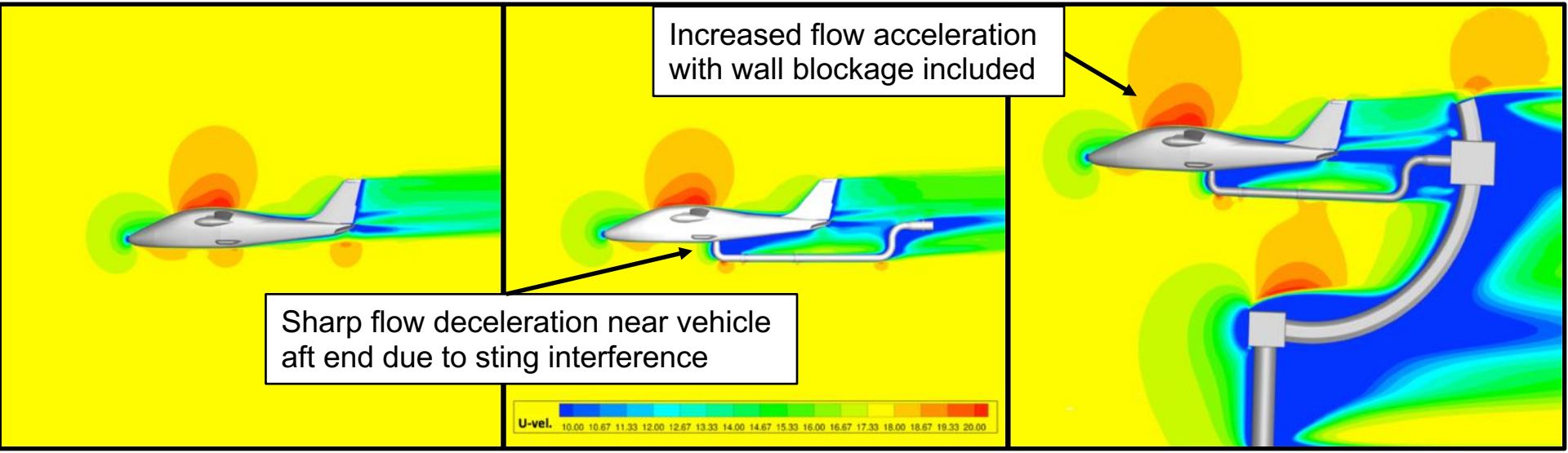

Free air | **Free air + sting** | **Free air + sting + wind tunnel**

Validation Simulation Results (C_p Contours on Aircraft Surface)

- Substantial qualitative differences in fluid dynamics resulting from sting, C-strut and wind tunnel walls
- Hardware locally impacts flow field while effects also propagate upstream to test article location

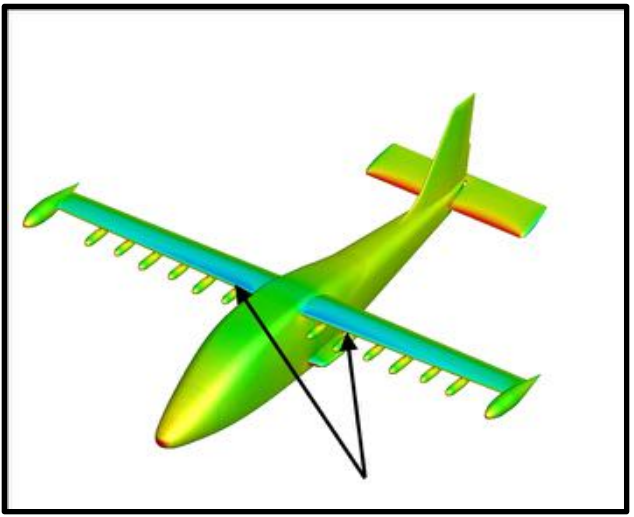

Free air

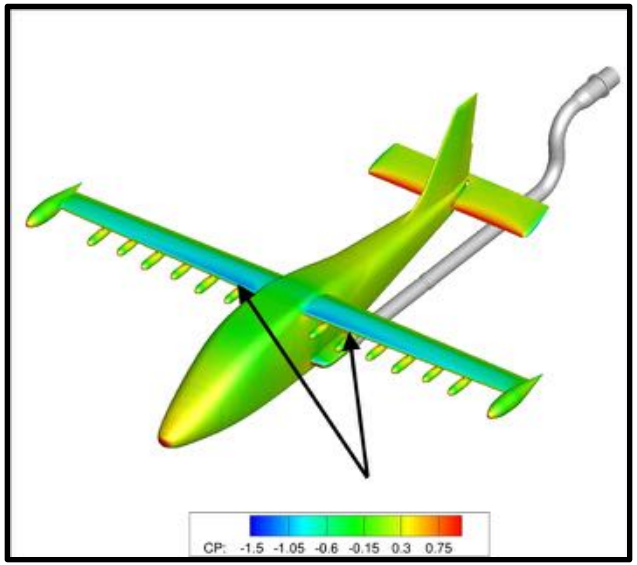

Free air + sting

Increased flow acceleration over upper surface creates suction-induced lift

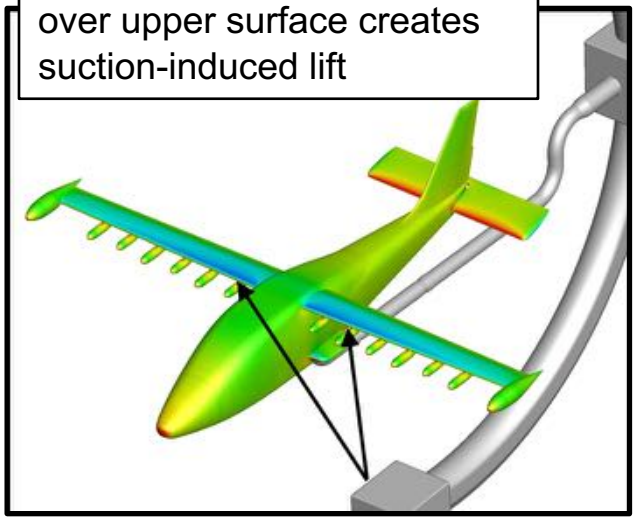

Free air + sting + wind tunnel

Build-Up Simulation Results

- Pressure distribution at a selected spanwise wing location is compared for each build-up level
- Progressively increased pressure differential is seen as components are added
- Slight impact with the addition of sting and most substantial impact occurs with the wind tunnel walls

Case	C_L	% err. C_L
Free Air	0.4575	20.6
Free Air + Sting	0.4782	17.8
Wind Tunnel + Sting + C-strut	0.5394	6.4
Experiment	0.5762	-

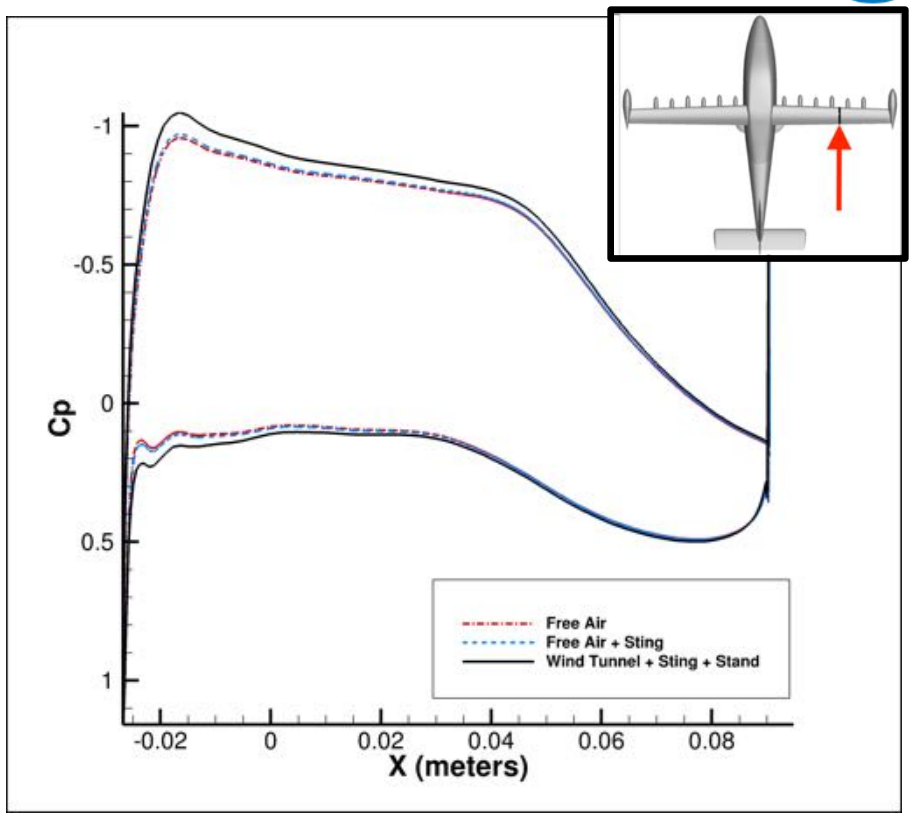

Build-Up Simulation Results

- Most substantial reduction of error is seen through lift coefficient, where free-air modeling error of 20.6% was reduced to 6.4% for LAVA Curvilinear when simulated appropriately
- Negligible change in drag error relative to experiment

	LAVA Curvilinear				Star-CCM+ Unstructured			
Case	C_L	% err. C_L	C_D	% err. C_D	C_L	% err. C_L	C_D	% err. C_D
Free Air	0.4575	20.6	0.0970	9.4	0.4691	18.6	0.1003	6.3
Free Air + Sting	0.4782	17.8	0.1003	6.3	-	-	-	-
Wind Tunnel + Sting + C-strut	0.5394	6.4	0.0977	8.8	0.5307	7.9	0.0999	6.7
Experiment	0.5762	-	0.1071	-	0.5762	-	0.1071	-

Additional Angle of Attack Sweep

- Comparison of multiple angles of attack in free air and with wind tunnel hardware further demonstrate modeling impacts
- For both codes, incorporating wind tunnel effects to the CFD simulation improve lift predictions considerably across the linear regime of the C_L vs. α curve
- Changes observed for drag and pitching moment, however no considerable change in accuracy

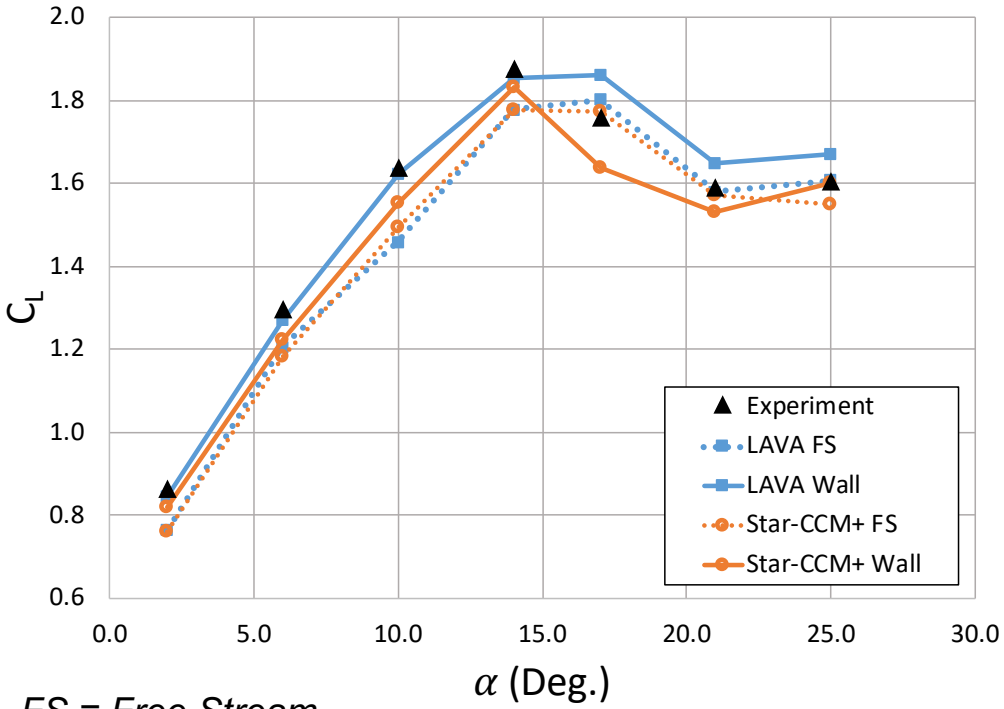

FS = Free Stream
Wall = Wind Tunnel + Sting + C-strut

Additional Angle of Attack Sweep

- Minor changes noted in drag and pitching moment in the pre-stall regime, but no significant change in error relative to experiment
- Larger scatter in results observed post-stall independent of modeling approach

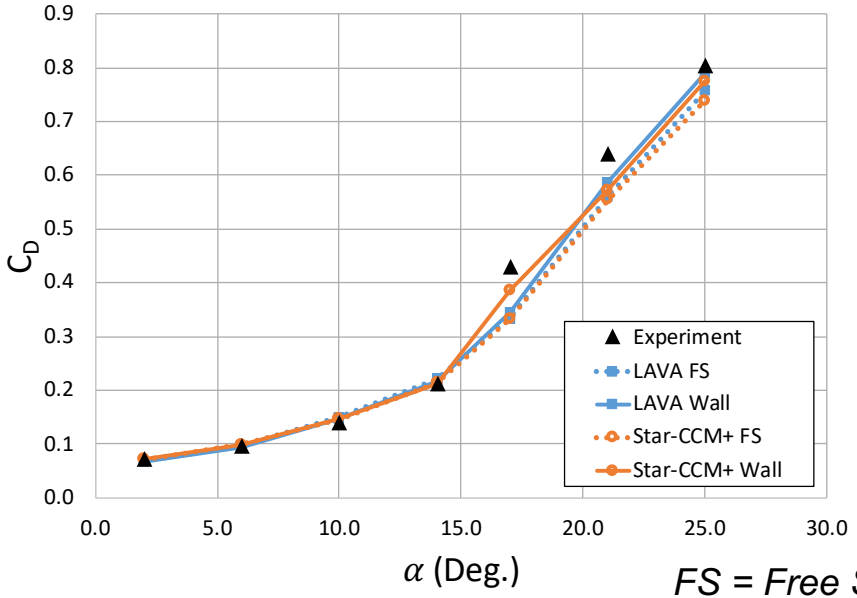

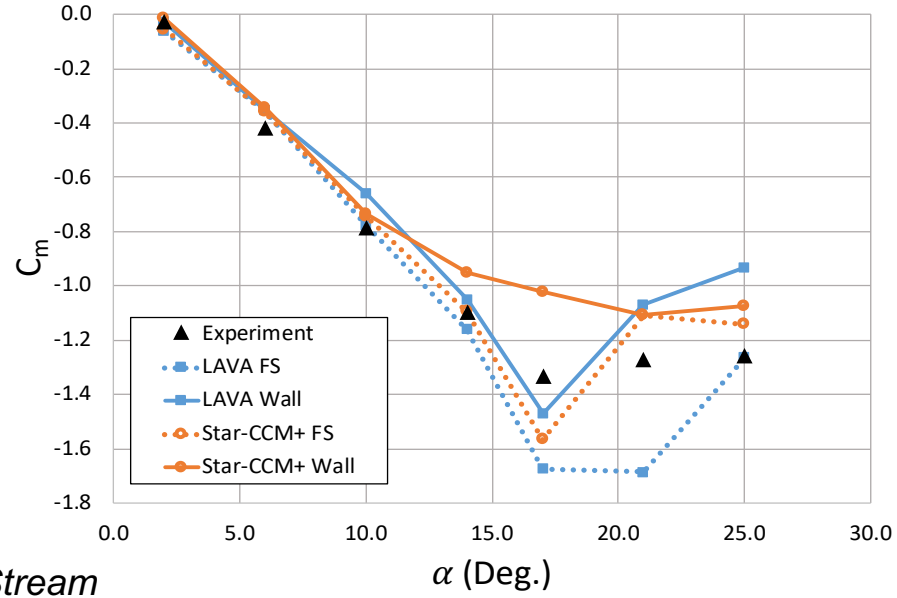

FS = Free Stream
Wall = Wind Tunnel + Sting + C-strut

Outline

- Introduction
  - X-57 CFD task overview
  - Motivation
- Part I: Computational simulations without propulsion
  - Establishing CFD Best Practices
    - Grid generation
    - Mesh refinement study
    - Numerical methods
    - Wind tunnel validation study
  - Power-Off Aerodynamic Database Results
- Part II: Computational simulations with propulsion
  - Cruise Power-On Database
  - High-Lift Power-On Database
- Summary

Database Execution

- Findings from mesh refinement and modeling approach studies are then applied to the power-off aerodynamic database (188 RANS runs)
  - Models flight performance for three flap settings
    - Take-off (10º deflection)
    - Cruise (0º deflection)
    - Landing (30º deflection)
- Preliminary results for nominal cruise setting are presented in the following slides, more detailed database results will be presented in future publications

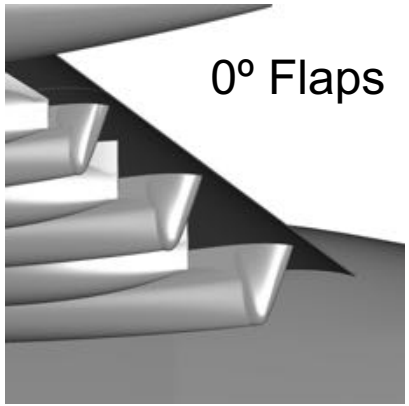

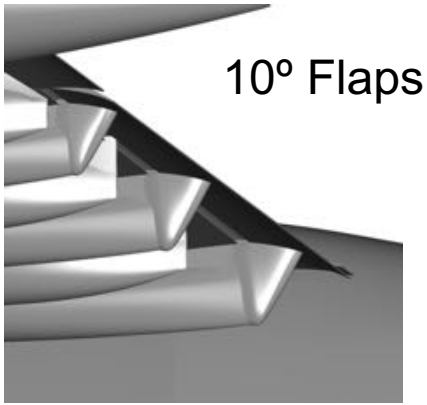

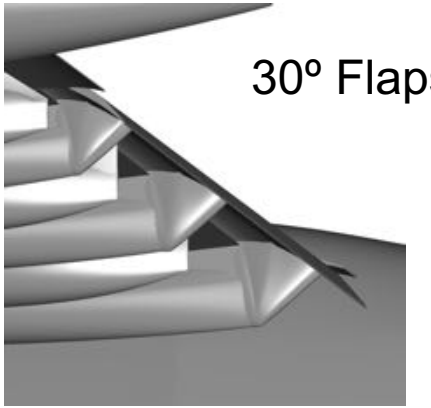

AoA Sweep at Cruise Condition

- Updates to existing wind tunnel grid were made to reflect new high-lift pylon design and added vortex generator
- Angles of attack were selected to determine aerodynamic performance with all control surfaces at their nominal position

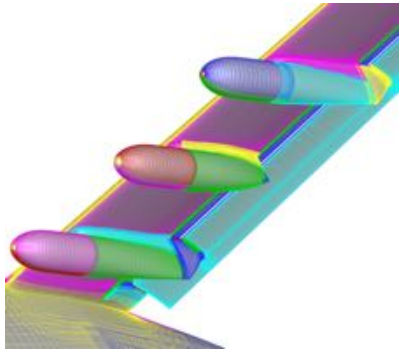

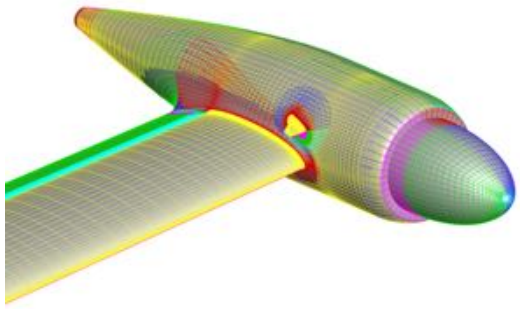

Grid Points: 139 M
Zones: 333 grids

Quantity	Value
Mach Number	0.233
Reynolds Number based on MAC	2,790,000
Reference Static Temperature	288.1 K
Sideslip Angle	0.0 º
Aileron Deflection	0.0 º
Rudder Deflection	0.0 º
Stabilator Deflection	0.0 º
Flap Deflection	0.0 º

Cruise Condition AoA Sweep Results

- LAVA predicts lift within 0.5% of Star-CCM+ for pre-stall AoA, and within 8% post-stall
- This level of agreement is a result of the work completed prior to the database
- RANS simulations after the stall angle of attack require higher fidelity models (e.g., LES, hybrid RANS/LES, etc.). Current simulation methods are not valid in this regime*

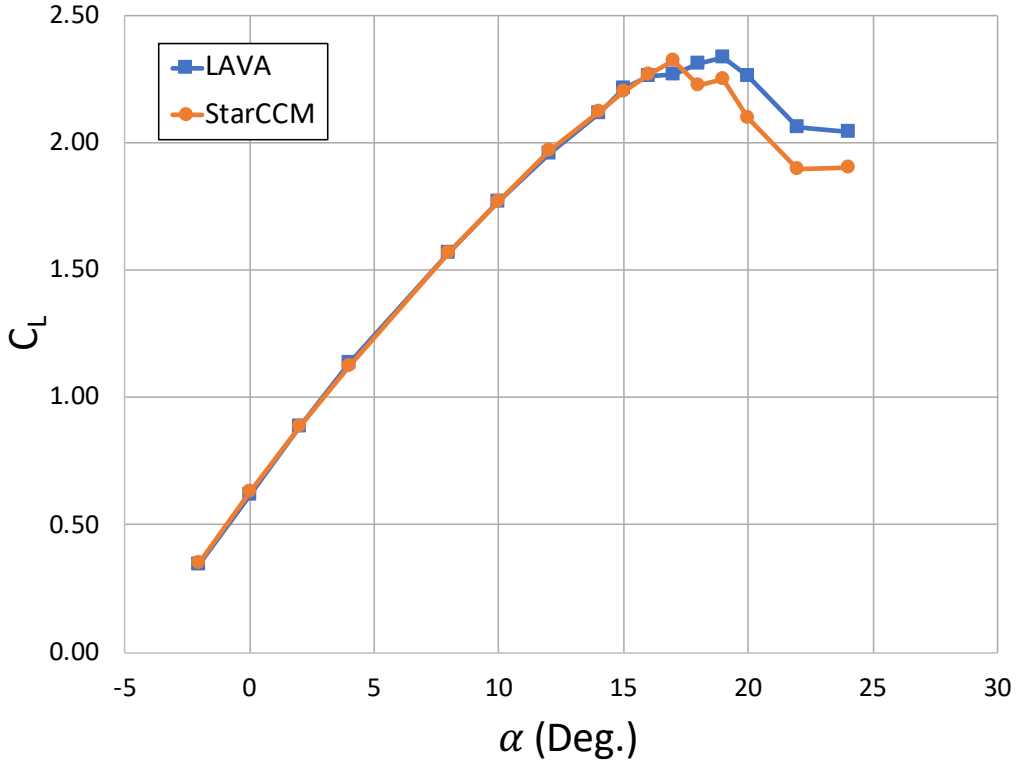

*Rumsey, C. L., Slotnick, J. P., and Sclafani, A. J., "Overview and Summary of the Third AIAA High Lift Prediction Workshop," 2018 AIAA Aerospace Sciences Meeting, 2018, p. 1258.

Cruise Condition AoA Sweep Results

- LAVA Curvilinear and Star-CCM+ predict drag and pitching moment within 5% of each other pre- and post-stall

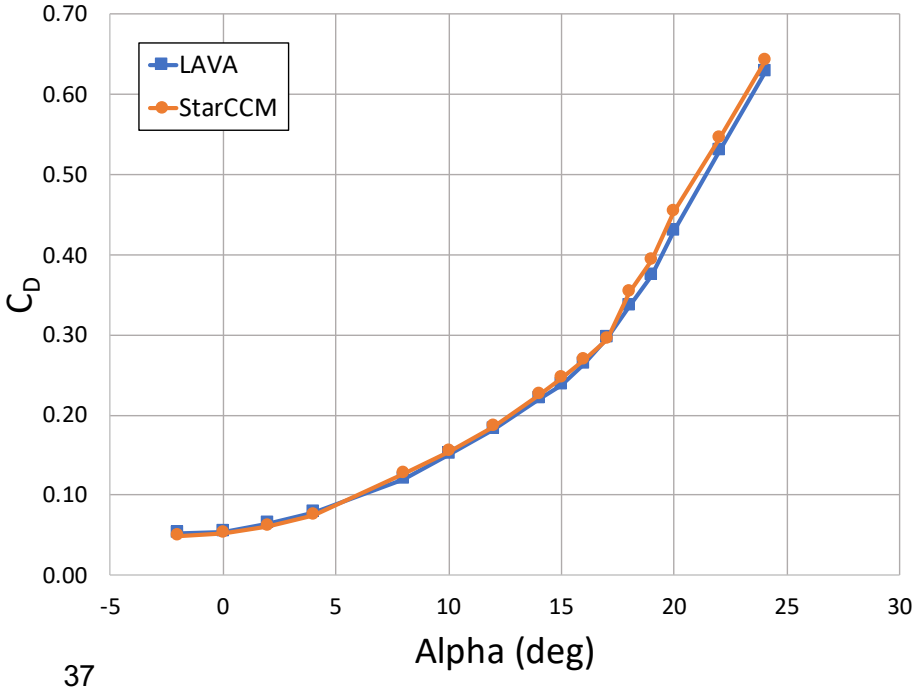

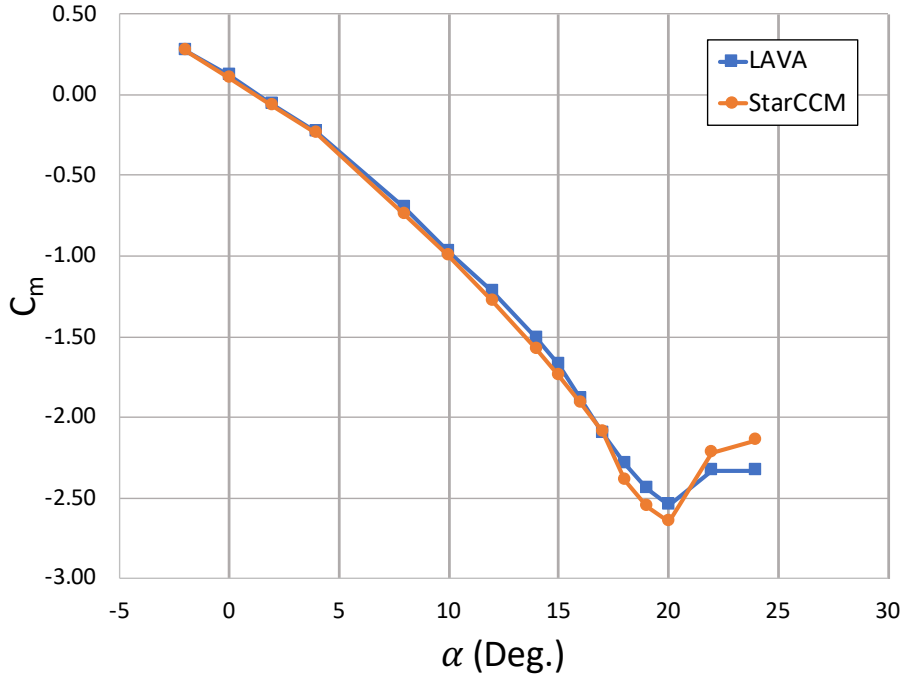

Cruise Condition AoA Sweep Results

- Closer examination of flow structures at selected angles of attack confirm the similar predictive capabilities of LAVA Curvilinear and Star-CCM+
  - ***Note: Particle seeding for streamlines randomly distributed for each figure***
- Pre-stall angles of attack predict attached flow with minor separation developing at high-lift pylon locations

16º angle of attack, LAVA Curvilinear

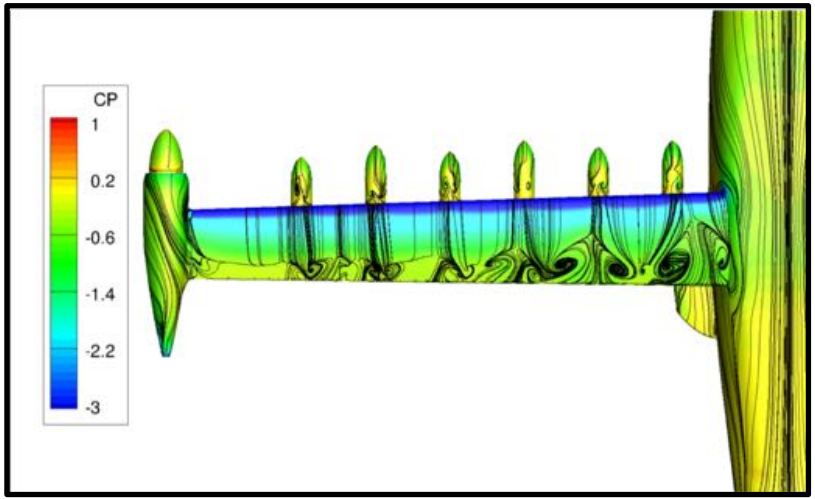

16º angle of attack, Star-CCM+

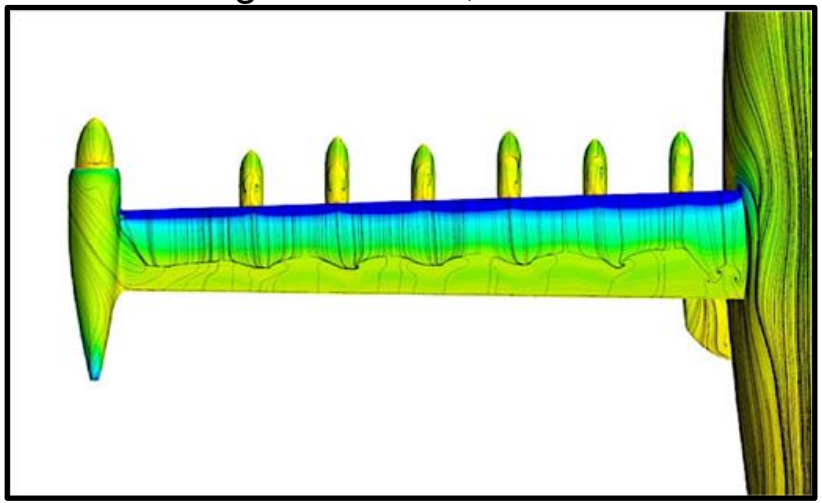

Part I Summary

- Establishing best practices prior to database generation is an important step to ensure success in future simulations
  - Develop efficient mesh generation techniques
  - Determine refinement level
  - Determine numerical schemes
  - Validate against experimental data
- Properly establishing these best-practices minimizes the CFD error and can be applied to similar geometries
  - Proper simulation techniques can potentially reduce CFD error relative to experiment from above 20% to about 6% as shown with lift coefficient
  - Code-to-code error in aerodynamic loads as low as 0.5% was observed, as well as a prediction of $C_{L,max}$ within 0.6%
- These concepts will be applied to X-57 simulations that include propulsion

Outline

- Introduction
  - X-57 CFD task overview
  - Motivation
- Part I: Computational simulations without propulsion
  - Establishing CFD Best Practices
    - Grid generation
    - Mesh refinement study
    - Numerical methods
    - Wind tunnel validation study
  - Power-Off Aerodynamic Database Results
- Part II: Computational simulations with propulsion
  - Cruise Power-On Database
  - High-Lift Power-On Database
- Summary

Power-On Simulation Preparation

- Best practices from the power-off CFD database preparation were also applied to power-on database simulations
  - Mesh refinement studies
  - Numerical scheme/turbulence model determination
  - Code-to-code comparison
- Refinement level and numerical schemes/models identical to power-off simulations deemed adequate
- Additional studies need to be performed to determine best propulsion modeling approach

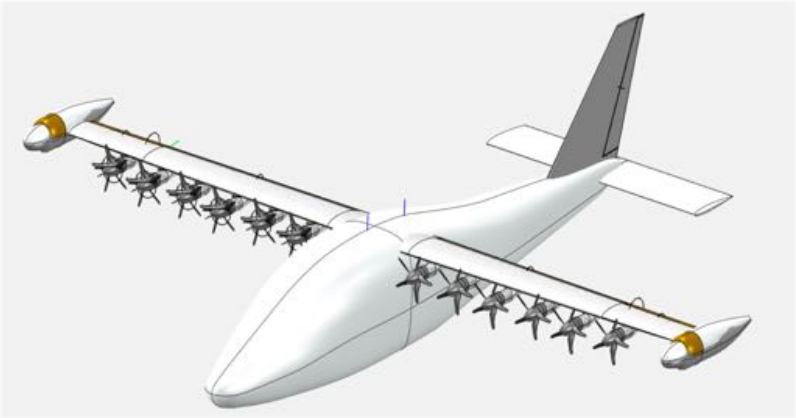

Modeling High-Lift and Cruise Propeller Propulsion

- Developing the X-57 flight simulator requires quantifying the aerodynamic loads for a variety of power-on flight scenarios
  - Cruise propellers only
  - High lift propellers only
  - Failure scenarios
- Mod-III and Mod-IV power-on aero databases study the effects of propulsion and quantify the "*aero deltas*" relative to power-off simulations

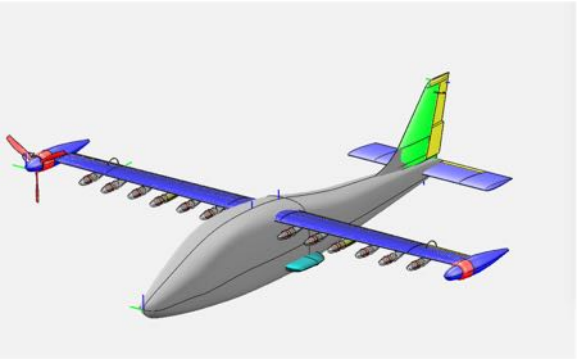

Cruise propellers (Mod-III)

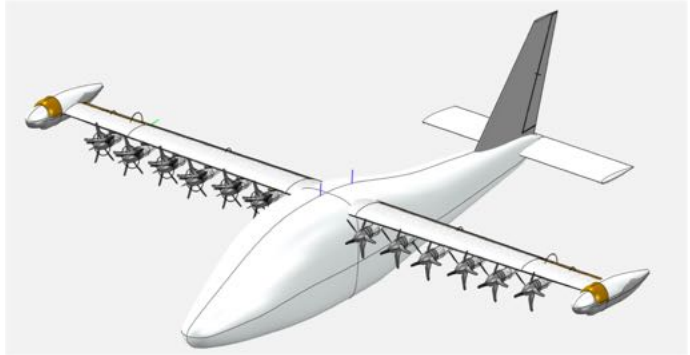

High lift propellers (Mod-IV)

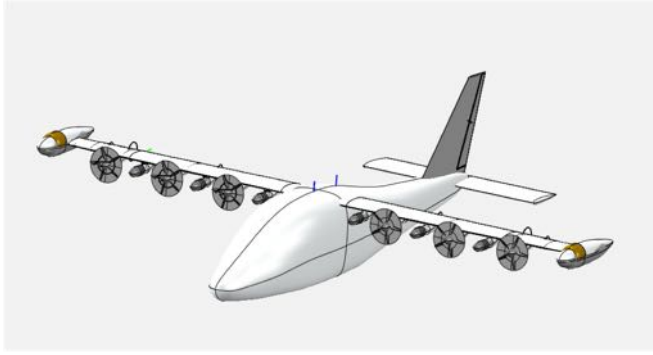

Bus failure scenario (Mod-IV)

Propulsion Modeling Approach

- *Actuator zones* model the momentum imparted from the propeller to the surrounding flow field without the computational cost of simulating the moving blade
- Axial forces (thrust) and tangential forces (torque) as a function of propeller radius are needed to define the actuator zone model
- Radial thrust and torque distribution options studied with LAVA
  - Constant
  - Goldstein Optimum[1]
  - Arbitrary

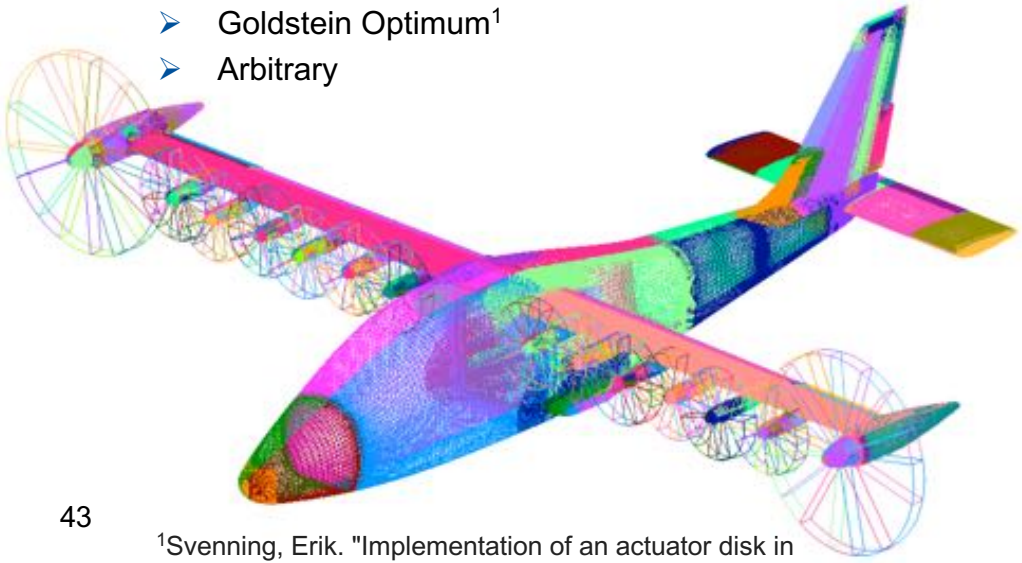

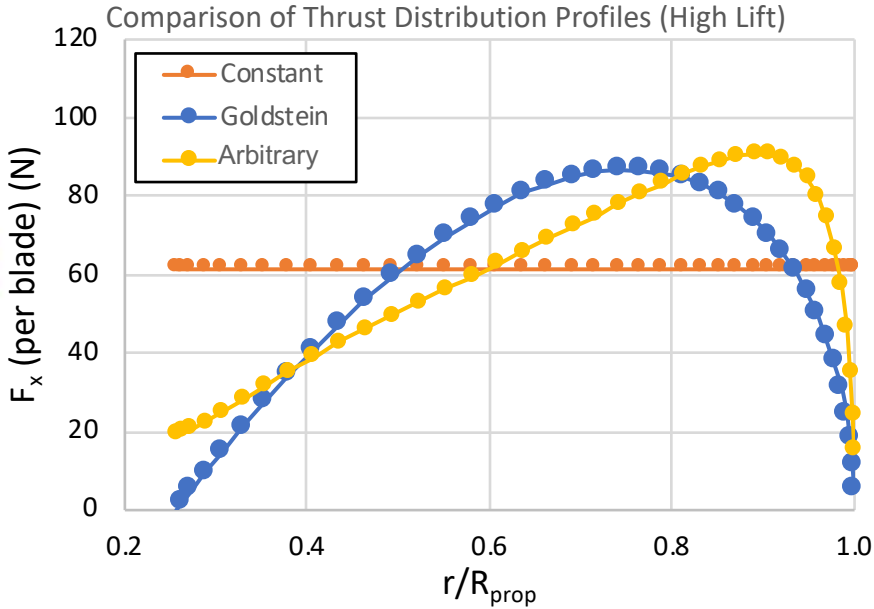

[1]Svenning, Erik. "Implementation of an actuator disk in OpenFOAM." *(Chalmers University of Technology, Sweden, 2010)* (2010).

Outline

- Introduction
  - X-57 CFD task overview
  - Motivation
- Part I: Computational simulations without propulsion
  - Establishing CFD Best Practices
    - Grid generation
    - Mesh refinement study
    - Numerical methods
    - Wind tunnel validation study
  - Power-Off Aerodynamic Database Results
- Part II: Computational simulations with propulsion
  - Cruise Power-On Database
  - High-Lift Power-On Database
- Summary

Cruise Power-On Simulation Method

- Similar preparations were performed for power-on simulations as power-off
  - Mesh refinement study
  - Numerical dissipation
  - Turbulence model corrections
- Selected solver settings
  - Steady-state RANS
  - Second-order convective flux with Koren limiter
  - SA turbulence with RC/QCR2000 correction enabled
- Actuator zone modeling
  - Cruise propellers are modeled with actuator zone source terms using the Goldstein radial thrust and torque distributions

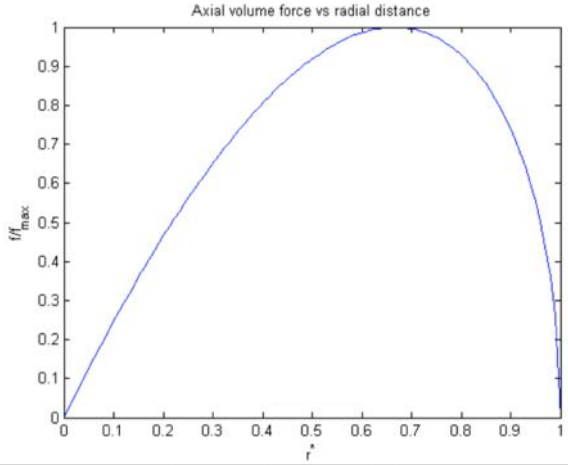

Thrust (Goldstein)

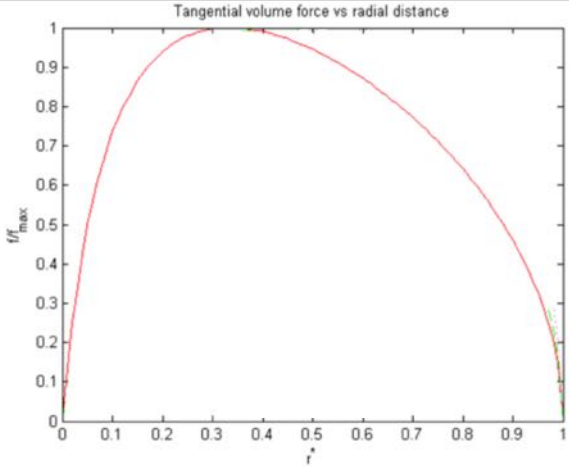

Torque (Goldstein)

Cruise Power-On Sample Simulations

- The Mod-III power-on database simulates 10 flight conditions, for each of which the control surfaces and power settings would be varied
- Power-off mesh modified to include actuator zone regions where the propulsion source term would be applied
- Sample results shown will be for the following condition
  - Altitude: 2,500 ft, V_∞ = 150.0 ft/s, Mach = 0.136, Re_{MAC} = 1,921,000

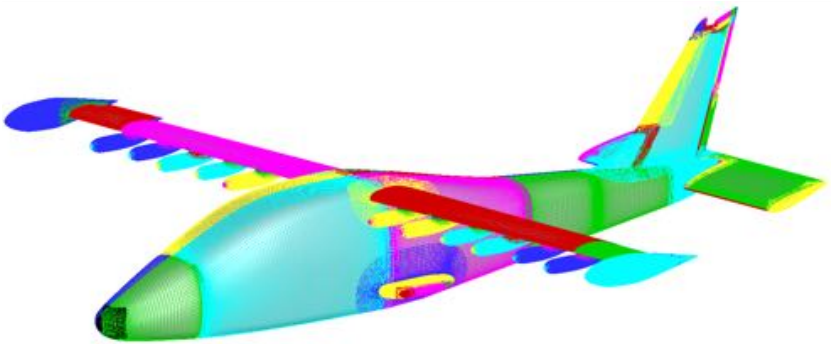

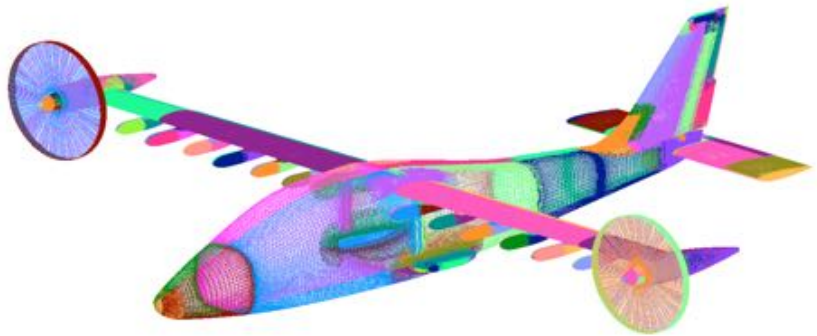

Grid points: 120.9 M

Grid points: 128.7 M

Cruise Power-On Simulation Sample Results

- Altitude: 2,500 ft, V_∞ = 150.0 ft/s, Mach = 0.136, Re_{MAC} = 1,921,000
- Lift increases linearly with angle of attack until near stall, and shifts upward with power setting
- Drag increases parabolically with angle of attack, and shifts downward with increased thrust and slightly upward near 16 degrees AoA around stall

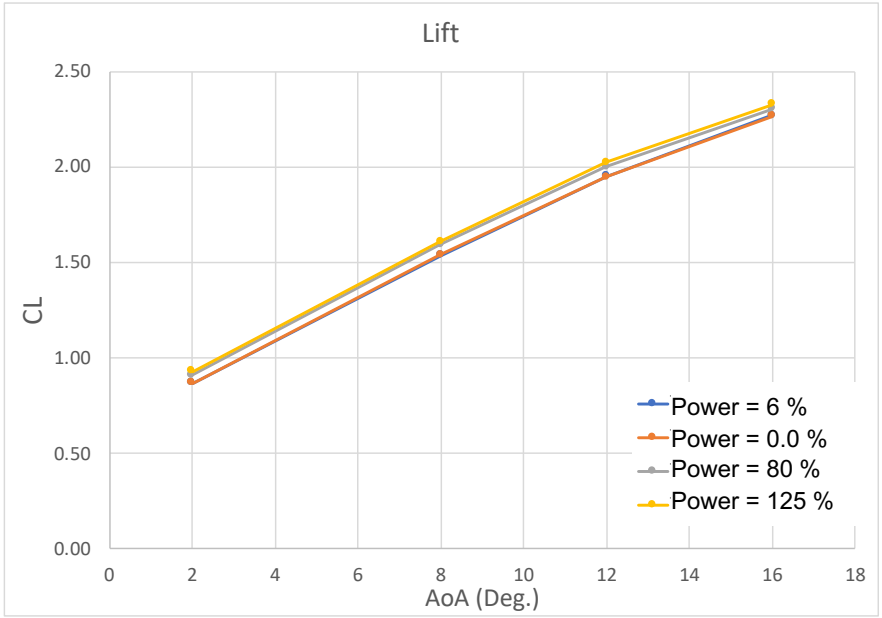

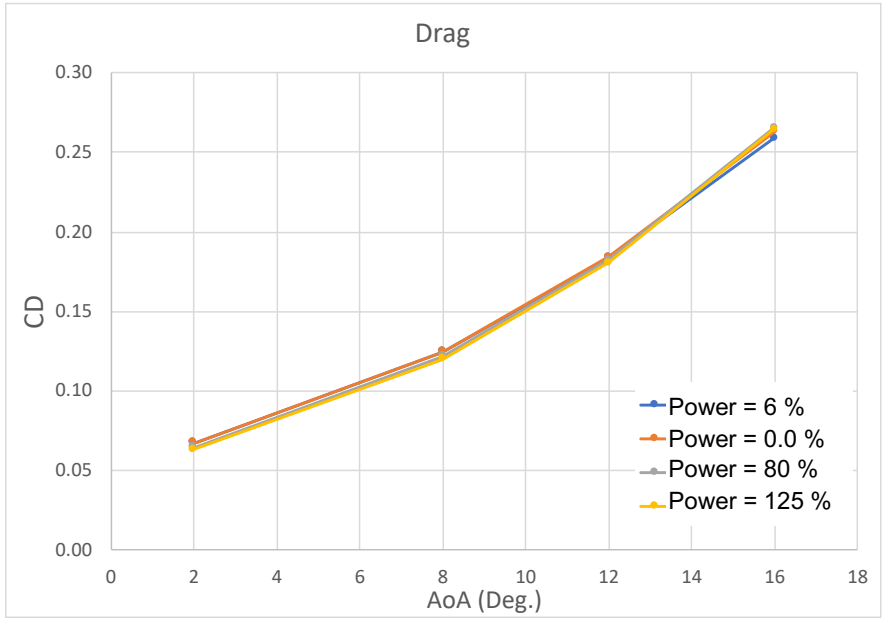

Cruise Power-On Simulation Sample Results

- Altitude: 2,500 ft, V_∞ = 150.0 ft/s, Mach = 0.136, Re_{MAC} = 1,921,000
- Nose-down pitching moment increases with applied thrust, and with angle of attack

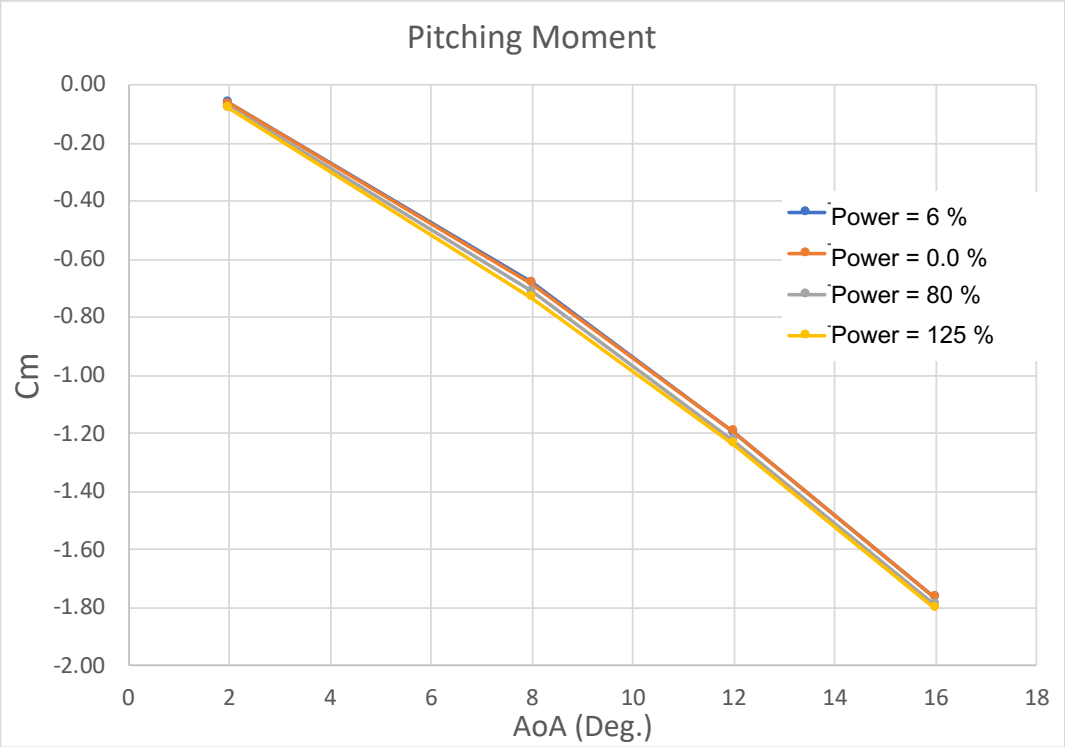

Cruise Power-On Flow Visualizations

- *Condition:* α = 12.0°, β = 0°, Altitude = 2,500 ft, V_∞ = 150.0 ft/s, Mach = 0.136, Re_{MAC} = 1,921,000
- Dimensionless streamwise velocity (U/U_{ref}) is shown on slice plane, pressure coefficient on aircraft surface

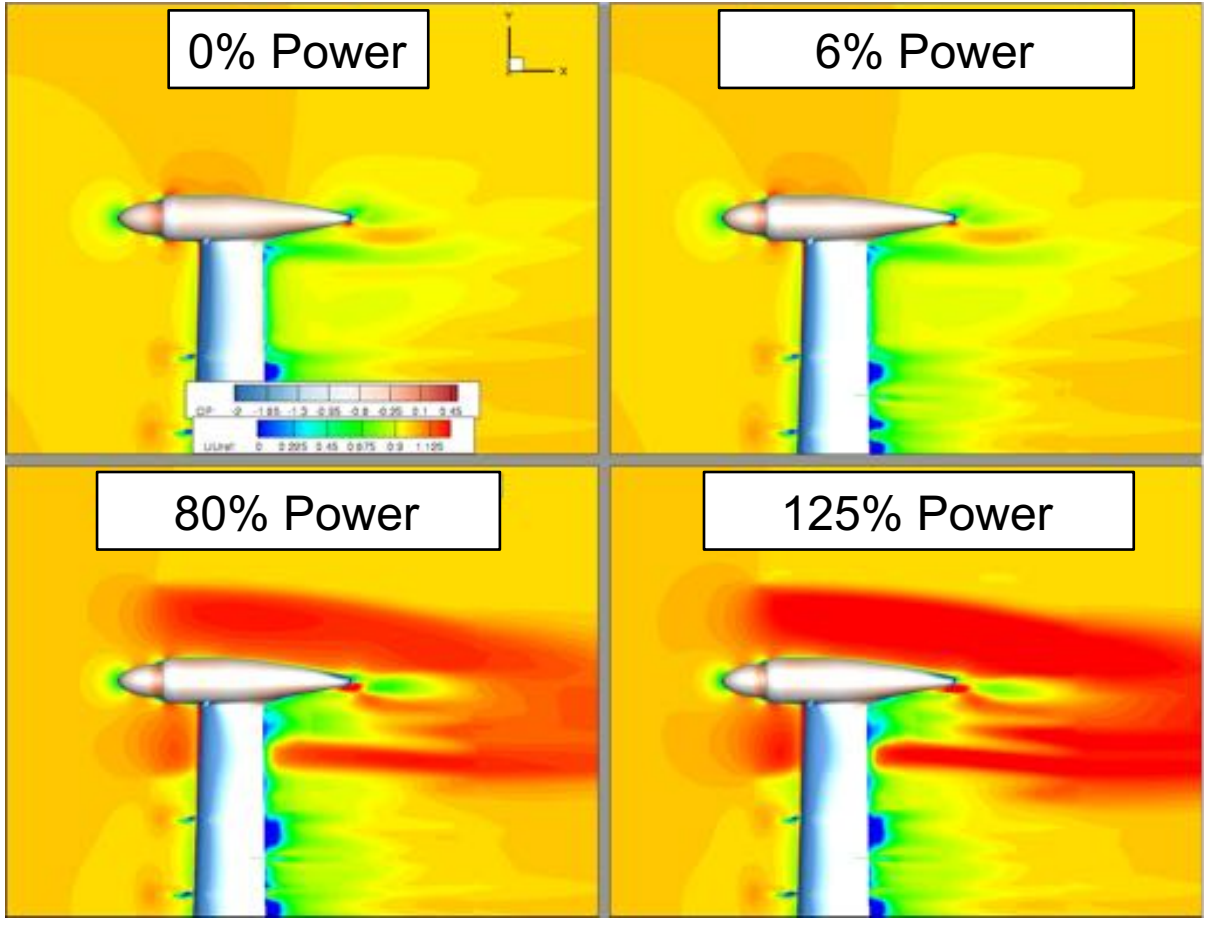

Cruise Power-On Flow Visualizations

- *Condition:* α = 12.0°, β = 0°, Altitude = 2,500 ft, V_∞ = 150.0 ft/s, Mach = 0.136, Re_{MAC} = 1,921,000
- Dimensionless streamwise velocity (U/U_{ref}) is shown on slice plane

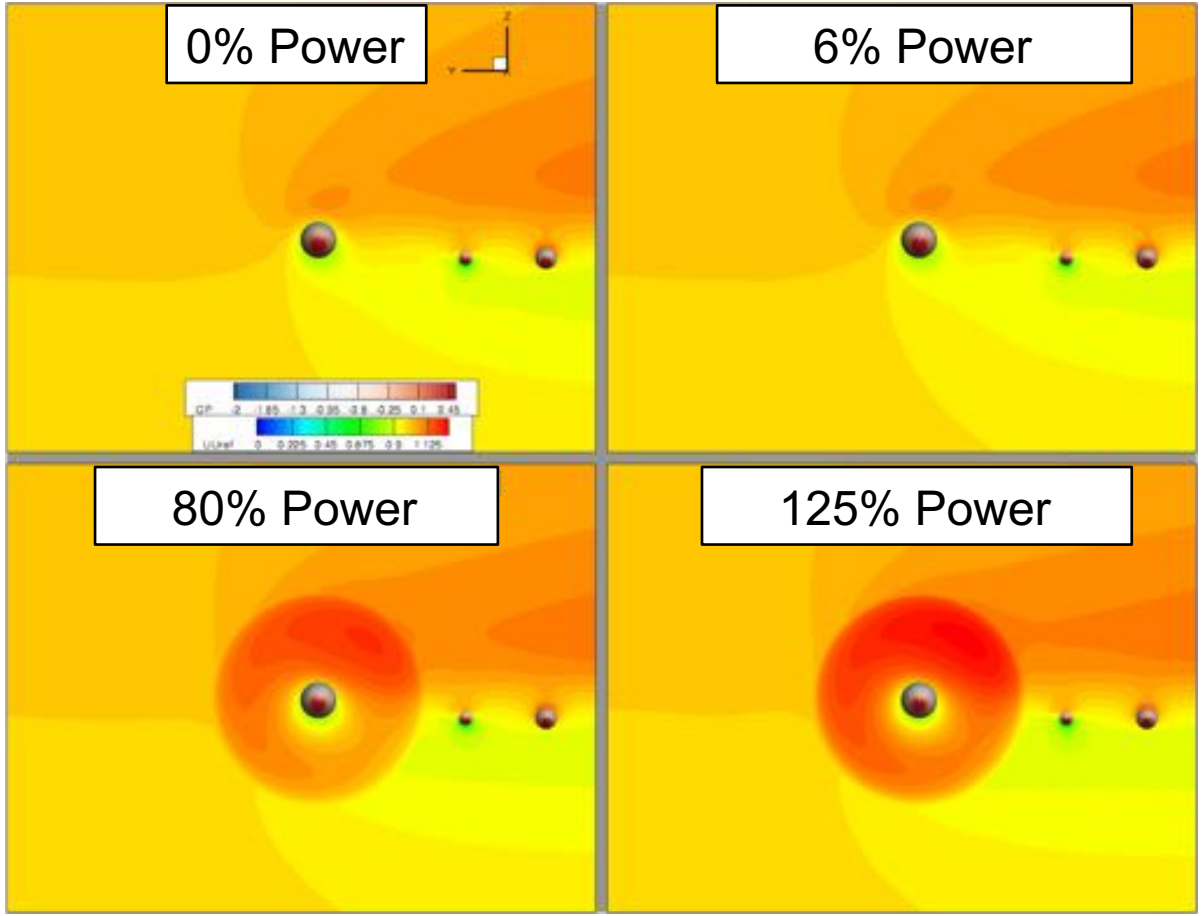

Outline

- Introduction
  - X-57 CFD task overview
  - Motivation
- Part I: Computational simulations without propulsion
  - Establishing CFD Best Practices
    - Grid generation
    - Mesh refinement study
    - Numerical methods
    - Wind tunnel validation study
  - Power-Off Aerodynamic Database Results
- Part II: Computational simulations with propulsion
  - Cruise Power-On Database
  - High-Lift Power-On Database
- Summary

Selecting Actuator Zone Distributions

- For high-lift propulsion cases, XROTOR[2] data was available to define an arbitrary radial thrust and torque distribution
- Initial CFD simulations were performed using LAVA to understand impact of thrust and torque distributions on the solution (Altitude: 6000 ft., Re_{MAC} = 1,235,000, Mach = 0.098, α = 10°)

Constant Thrust and Torque

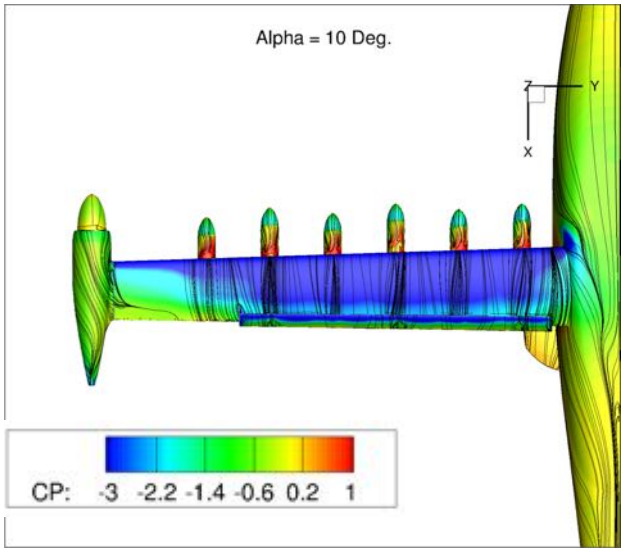

Goldstein Thrust and Torque

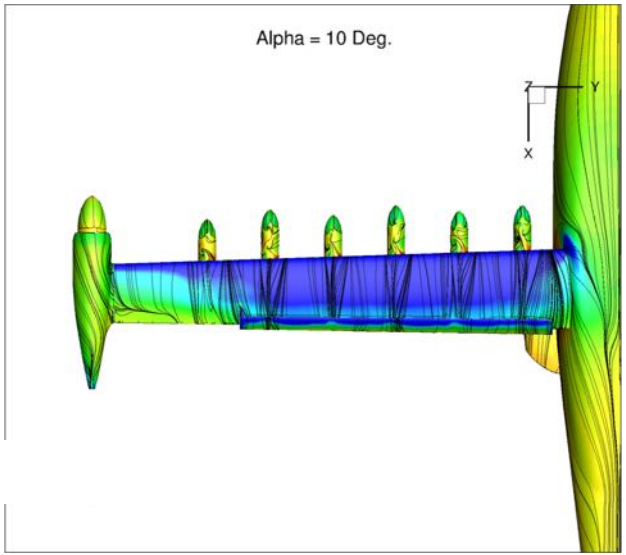

XROTOR Thrust and Torque

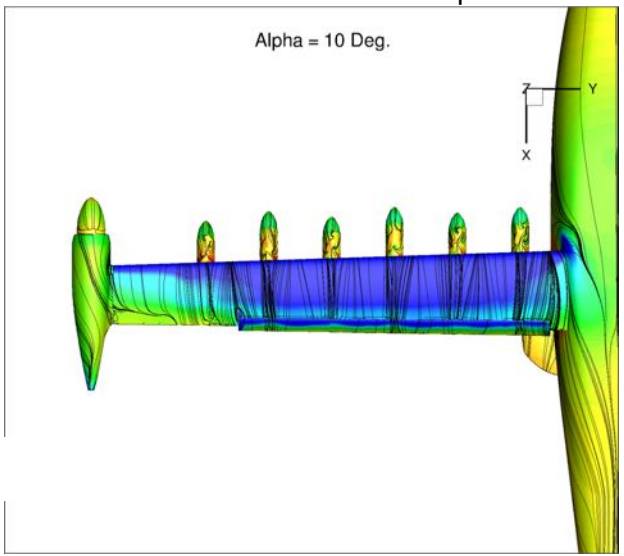

[2]Drela, M., and H. Youngren. "XROTOR: an interactive program for the design and analysis of ducted and free-tip propellers and windmills, 2011.[Software] Available at: http://web. mit. edu/drela."

Selecting Actuator Zone Distributions

- Initial CFD simulations were performed using LAVA to understand impact of thrust and torque distributions on the solution
- Altitude: 6000 ft., Re_{MAC} = 1,235,000, Mach = 0.098, α = 16^o shown below
- Separation behavior at high angle of attack highly dependent on thrust and torque distribution

Constant Thrust and Torque

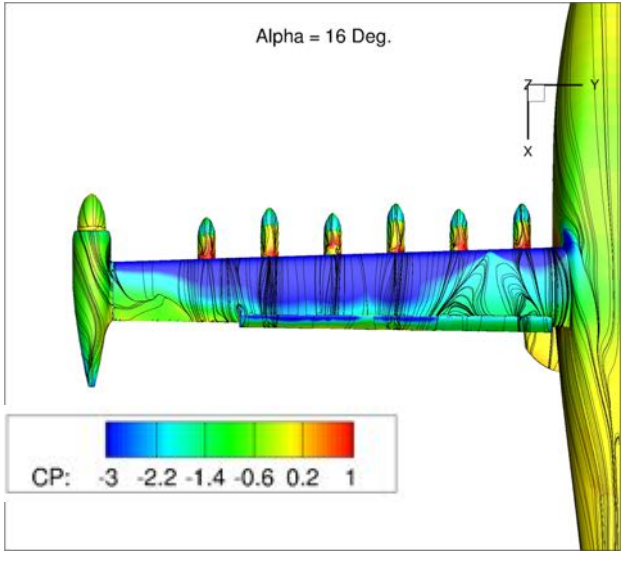

Goldstein Thrust and Torque

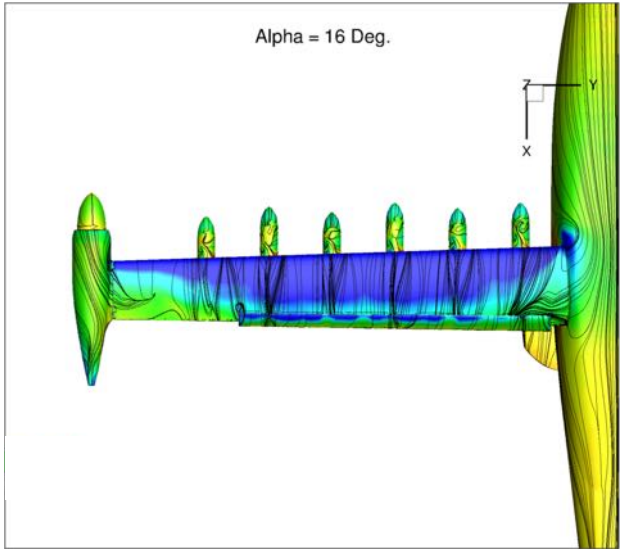

XROTOR Thrust and Torque

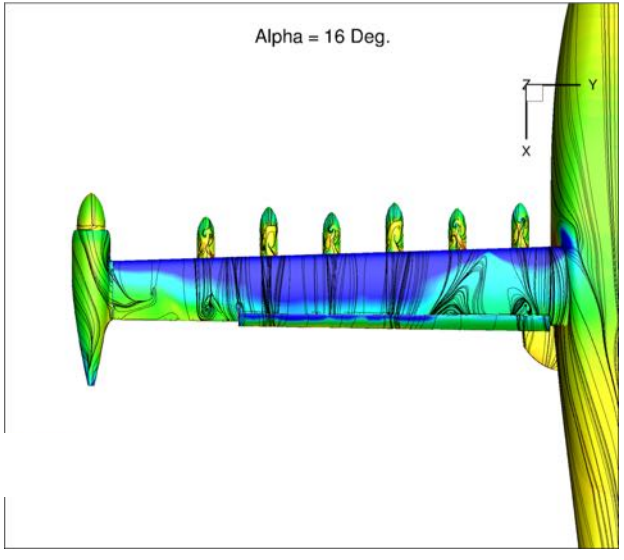

High-Lift Power-On Simulation Method

- Solver settings
  - Steady-state RANS
  - Second-order convective flux with Koren limiter
  - SA turbulence with RC/QCR2000 correction enabled
- Actuator zone modeling
  - All high-lift propellers are modeled with actuator zone source terms that utilize custom XROTOR radial thrust and torque distributions for a given flight condition
  - Sample distributions shown for 3,962 RPM, Mach 0.119, 2500 ft. altitude condition

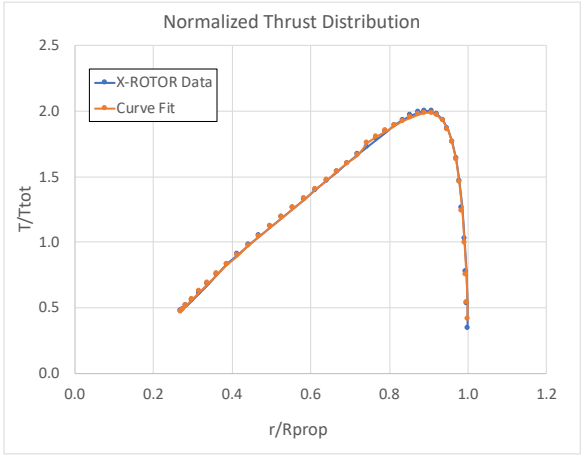

Thrust (X-ROTOR)

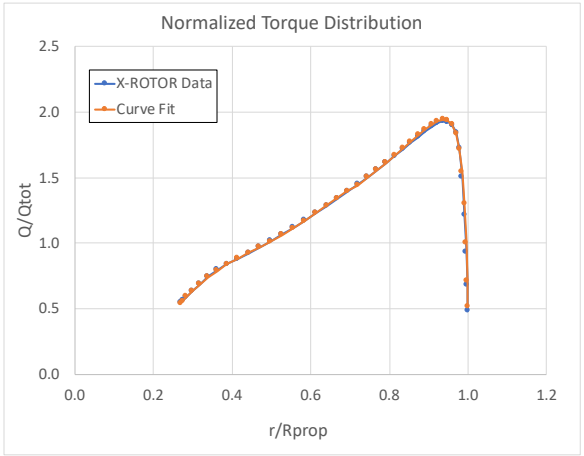

Torque (X-ROTOR)

High-Lift Power-On Power-On Sample Simulations

- The Mod-IV power-on database simulates 10 flight conditions, at which the control surfaces, flap deflections, and high lift power settings would be varied
- Power-off mesh modified to include actuator zone regions where the propulsion source term would be applied
- Sample results shown will be for the following condition
  - Altitude: 2,500 ft, Mach = 0.119, Re_{MAC} = 1,682,000, Flaps = 30°

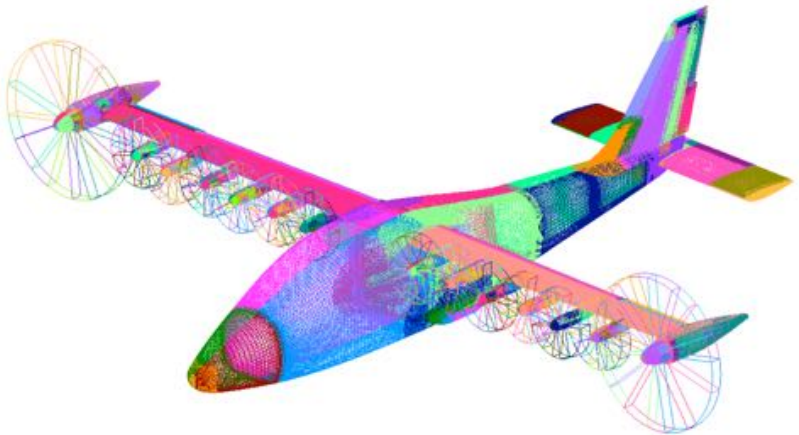

Grid points: 154.4 M

Grid points: 171.1 M

High-Lift Power-On Sample AoA Sweep Results

- Altitude: 2,500 ft, Mach = 0.119, Re_{MAC} = 1,682,000, Flaps = 30°
- Solid curves show high-lift power-on results, dashed curves show power-off for comparison
- LAVA predicts power-on lift within 1.4% of Star-CCM+ pre-stall, and within 8.5% post-stall
- LAVA predicts power-on drag within 3.1% of Star-CCM+ pre-stall, and within 5.7% post-stall

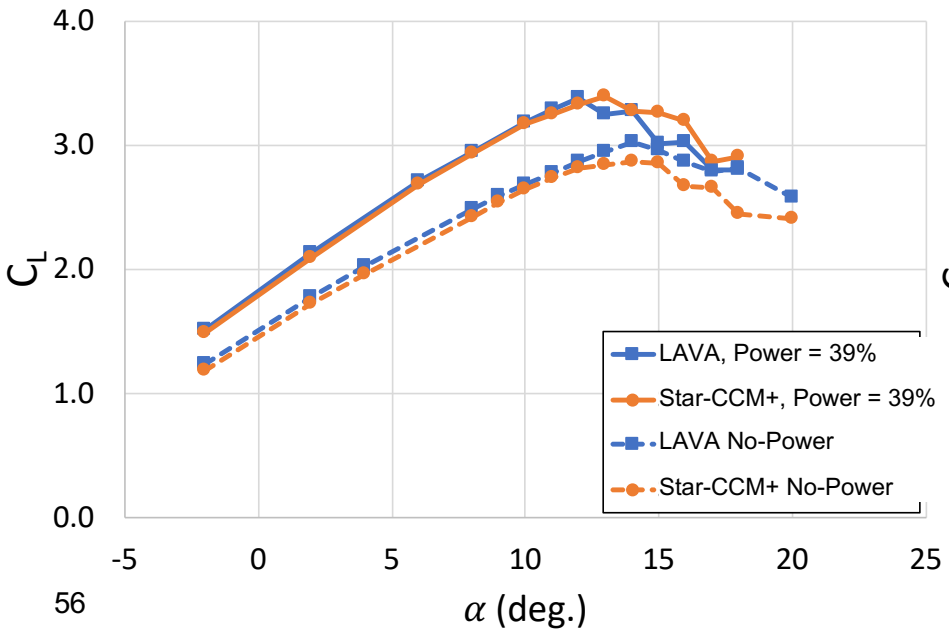

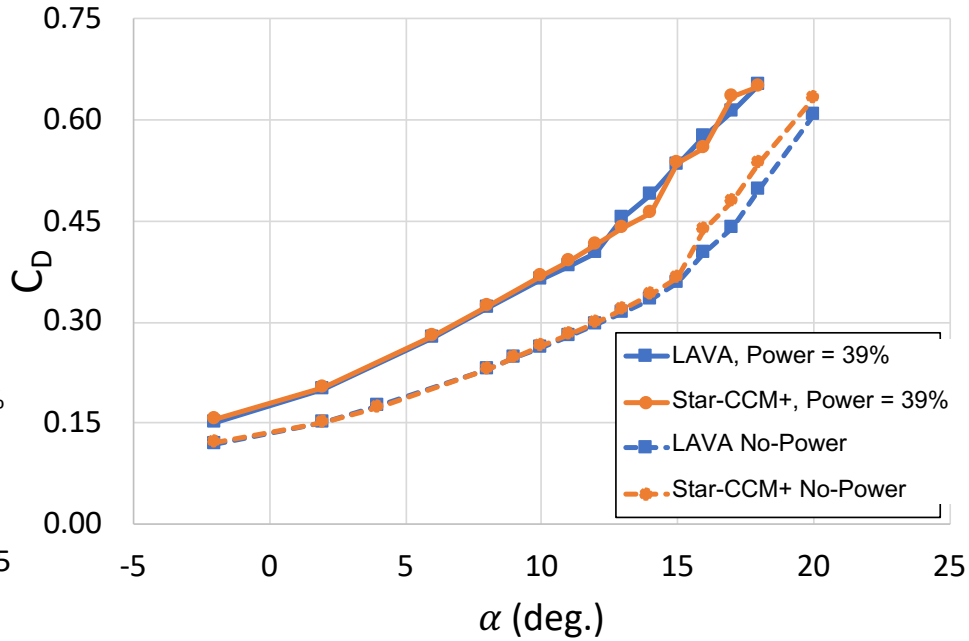

Part II Summary

- The best practices established during power-off simulations were applied to database simulations that include propulsion
  - Determined mesh refinement level
  - Determined numerical schemes
- Selected best propulsion modeling method
  - Thrust and torque distributions used for simulation have a large impact on flight performance, particularly near stall
- Strong code-to-code agreement pre-stall persists when propulsion is included in the simulation
  - Maximum difference in lift and drag between codes pre-stall for all high-lift motors powered on is observed to be 1.4% and 3.1%, respectively
  - $C_{L,max}$ value is predicted to within 0.4% and within ~1.0^{o} angle of attack

Summary of Resources Used

- LAVA Curvilinear
  - Intel Ivy Bridge E5-2680 Nodes on the Pleiades Supercomputer at NASA Ames Research Center
  - 1100-1200 cores were used for all computations presented here, with 900 cores for the ”coarse grid” cases and 1520 cores for the “fine grid” cases
  - Compute time: 12-16 hours/case
- Star-CCM+
  - Run on a cluster located at NASA Armstrong Research Center
  - Calculations performed on various node types and core counts depending on availability
  - 100k-200k cells per core were utilized on average
  - Compute time: 24-48 hours/case

Image source:
https://www.nasa.gov/centers/ames/news/releases/2010/10-45AR.html

Acknowledgments

- This project is funded by the Scalable Convergent Electric Propulsion Technology and Operations Research (SCEPTOR) program under the NASA Aeronautics Research Mission Directorate (ARMD)
- Michael Frederick and Trong Bui of the NASA Armstrong Aerodynamics and Propulsion Research Branch
- Experimental data provided by David Cox at NASA Langley Research Center
- Computer resources provided by NASA Advanced Supercomputing (NAS) Pleiades facility

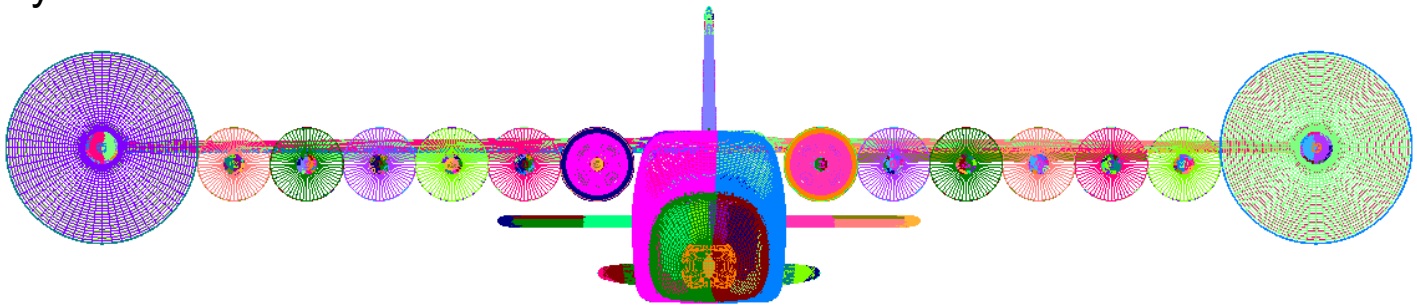

Questions?

Supplemental Slides

Cruise Condition AoA Sweep Results

- At stall, higher separation at 50% chord and aft predicted with both codes and exaggerated at high-lift pylon locations

4º angle of attack, LAVA Curvilinear

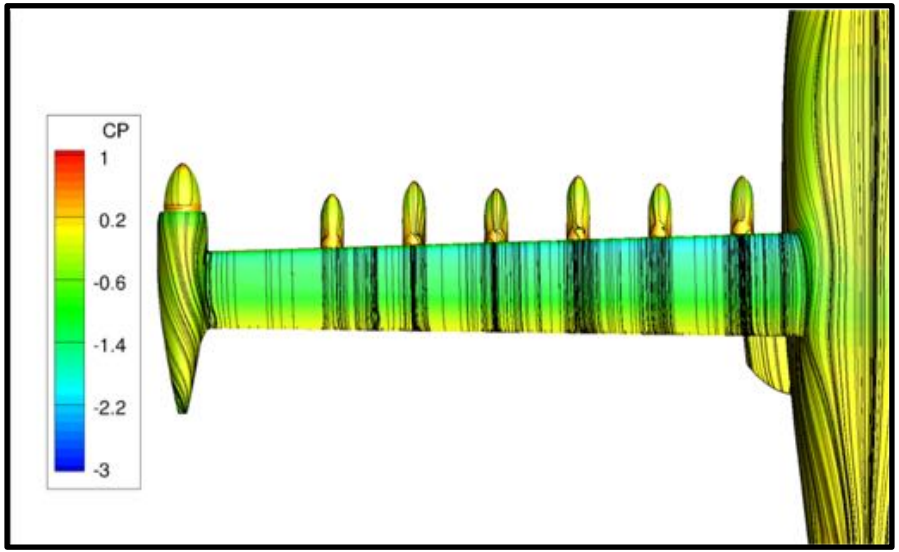

4º angle of attack, Star-CCM+

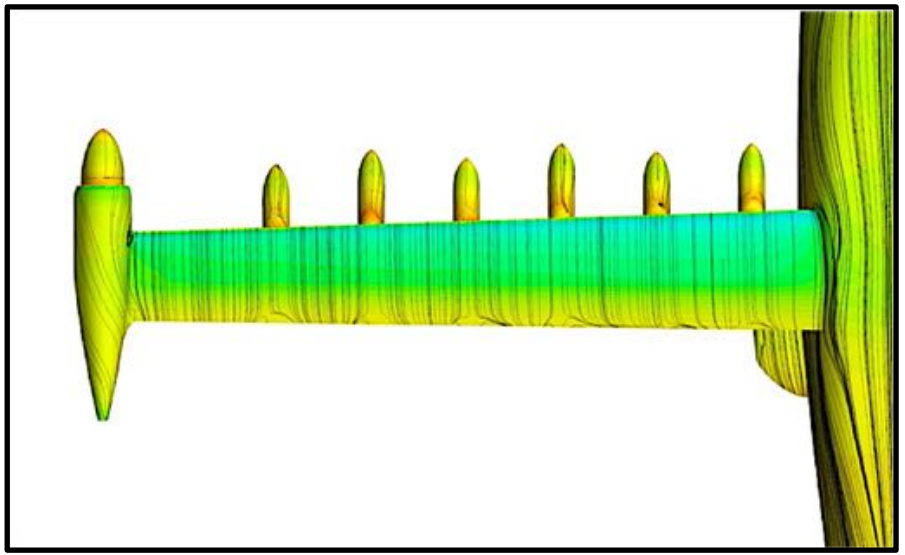

Cruise Condition AoA Sweep Results

- Post-stall, near total flow separation predicted for entirety of the wing with small pockets of attachment for both codes

22º angle of attack, LAVA Curvilinear

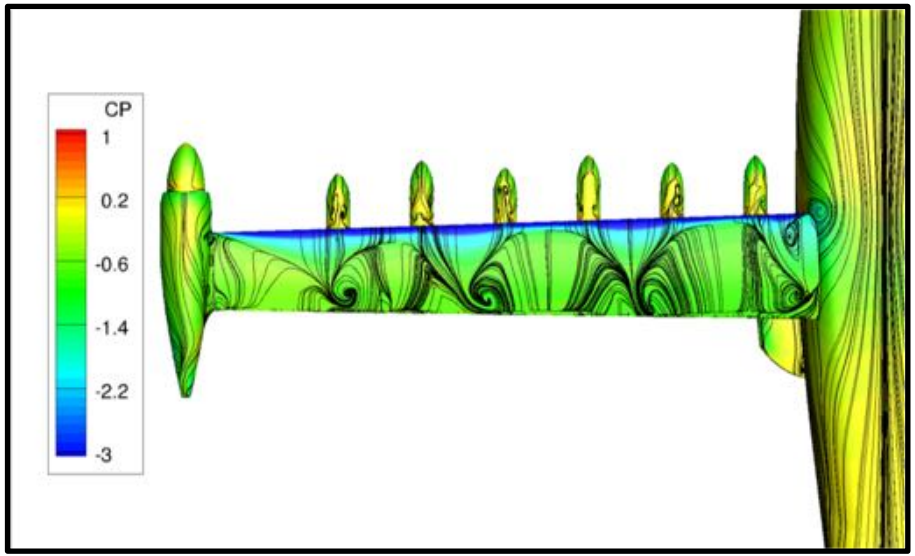

22º angle of attack, Star-CCM+